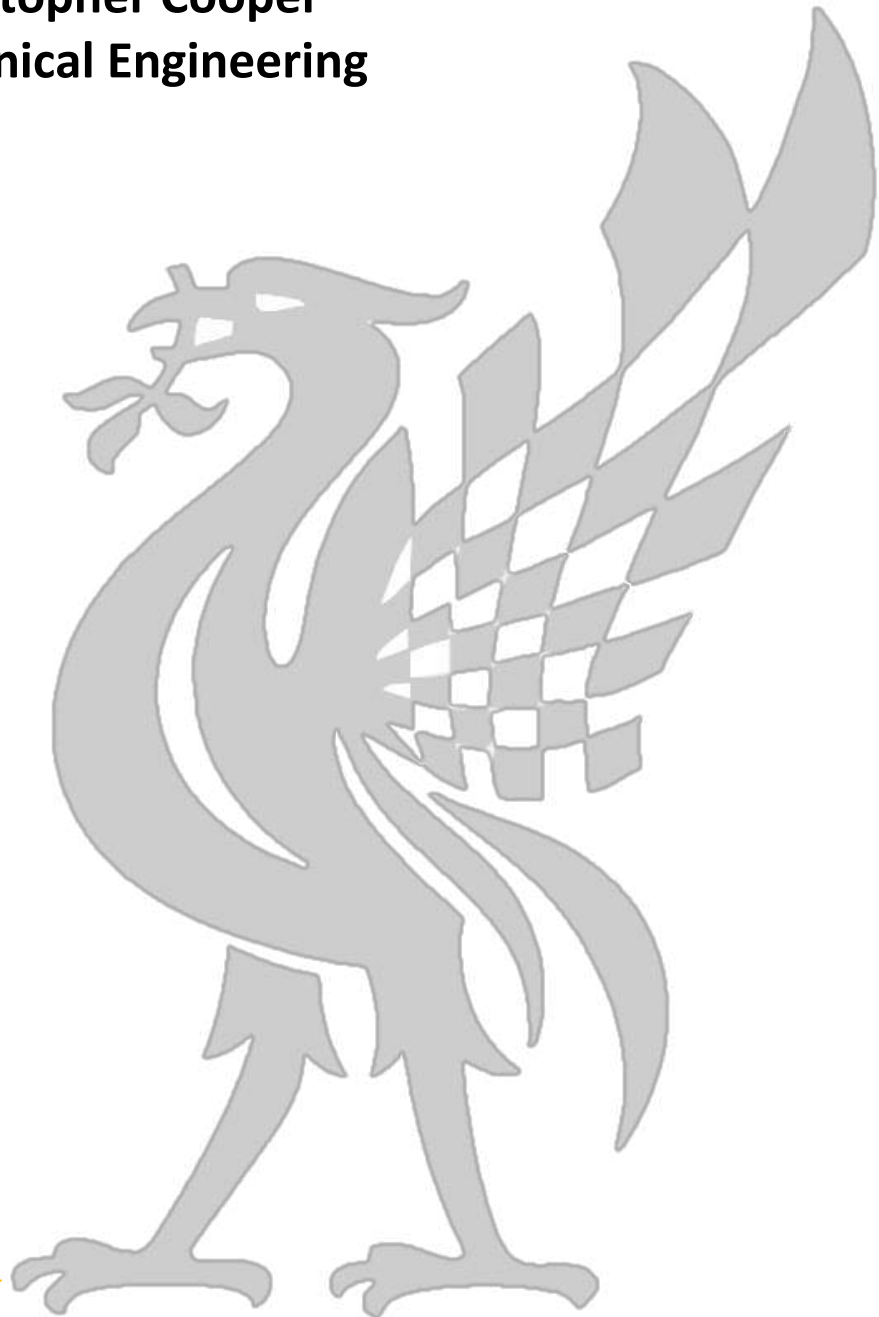


# **SCHOOL OF ENGINEERING FORMULA STUDENT**

**Design Methodology**

**ULM016 Chassis.**

**Christopher Cooper  
Mechanical Engineering**





## Summary

This report details the design process of ULM016's carbon fibre monocoque chassis. The faceted aluminium mould for the ULM015 chassis was re-used for the ULM016 chassis. The goal was to minimise as many changes to the chassis as possible to reduce the lead time on the car. The layup construction, in terms of ply angles and number of layers was mostly kept the same to avoid testing new panels for the SES. With the transition from IC (internal combustion) to EV (electric vehicle) changes have been made to house the high voltage system in the engine bay. To prevent damage to the high voltage system, the engine bay must be water tight. However, the high voltage system must be air cooled. The report details a louvre vent design to provide an inlet and outlet to the engine bay to allow air flow while preventing water from passing into the engine bay. Another key parameter for the transition from IC to EV is obtaining a 50:50 weight distribution, as this is key to the car's success. Due to the four in-hub motors, this weight distribution will optimise handling in terms of stability and agility while maintaining lots of traction off the line.

### 3 Engineering Science

#### 3.1 Simple battery calculations and understanding

For a general understanding, when adding cells in series the voltage increases, the current stays the same and the capacity in mAh stays the same. When you add batteries in parallel, the voltage remains the same, the current increases and the capacity in mAh increases. The number of parallel connections in a battery is determined by the size of the module, as most modules are designed to only hold cells that are connected in parallel due to the limitation of the voltage output of the module. Therefore, if you had a larger dimension module, i.e. 8p module you would have a higher capacity than a 6p module. However, if you have a larger dimension module, less modules can fit within the chassis and there are then less series connections. The less series connection, the lower the voltage of the battery and therefore the lower the power output.

$$Power = Voltage \times Current \tag{1}$$

$$Capacity(kWh) = (capacity(mAh) \times Voltage)/1,000,000 \tag{2}$$

Figure 7 demonstrates the dimensions for the space within the chassis for a four and six segment battery. As an example, given the space within the chassis for a 6 segment and 8p module, figure 8 demonstrates the number of modules that would fit in the engine bay.

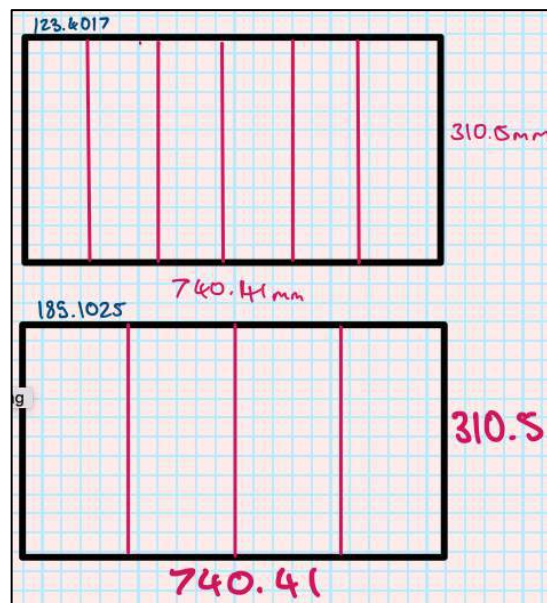


Figure 7 Dimensions of space in the engine bay ULM015.

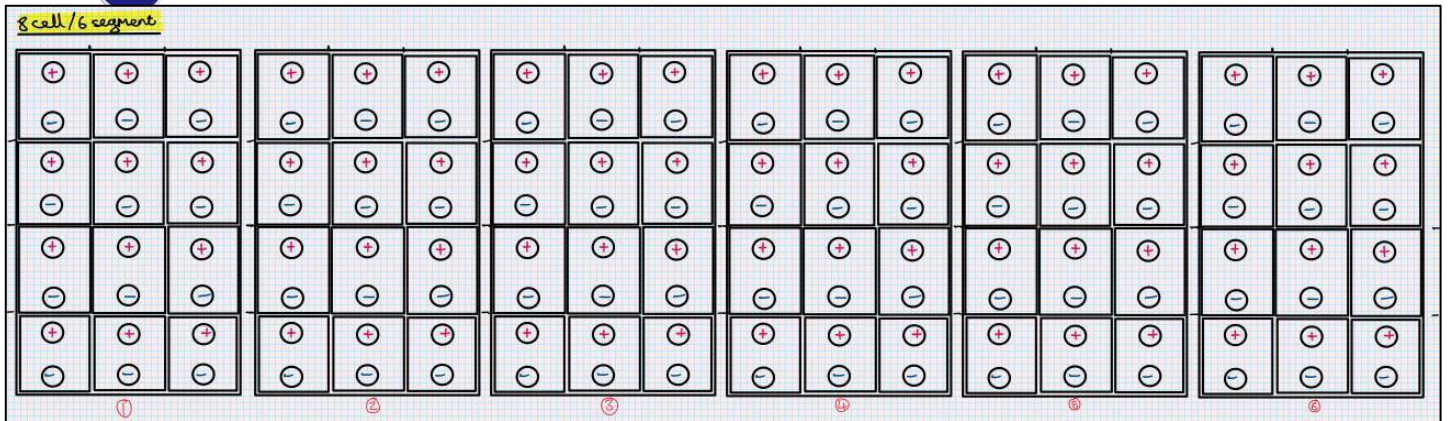


Figure 8 Number of 8p modules in chassis (72 series connections).

For a 3.6 volt nominal voltage cell with a capacity of 2800mAh, the calculations for the voltage and capacity (kWh) can be seen below.

$$\text{Voltage} = 72 \times 3.6 = 259.2V \tag{3}$$

$$\text{Capacity (kWh)} = \frac{(2800 \times 8) \times 259.2}{1,000,000} = 5.8kWh \tag{4}$$

The voltage and capacity for this arrangement of cells is too low for use with a 320kg electric vehicle with four motors. The capacity requirement for the battery was calculated to be approximately 7kWh.

### 3.2 Centre of mass

Another important parameter is the weight distribution and essentially the centre of mass. The height of and the location along the length of the car of the centre of mass can have significant effects on performance characteristics of the car. Centre of pressure from the aerodynamic force can also affect the performance of the car when working on conjunction with the centre of mass. The location of these parameters on the car can lead to oversteer and understeer due to the tyres becoming overloaded as shown in figure 5.

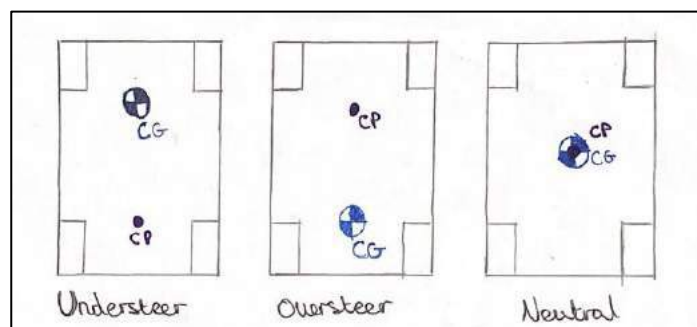


Figure 9 Centre of pressure and centre of mass (gravity) effect on handling.

Ideally, when cornering, the centre of pressure should align with the centre of mass to have the most tuned handling. However, depending upon the track, the car may perform better with more understeer (stability) or oversteer (agility). Stability will improve driver confidence as the car will be more self-correcting around corners but too much understeer will decrease the handling ability. Agility will do the opposite with increasing handling ability but the driver may have to do more corrections around corners (2). Traction off the line also has to be considered and as the ULM016 car is four-wheel drive the optimum ratio for traction would be 50:50 for front and rear axle. The calculation for the height and longitudinal length of the centre of mass can be seen below. This calculation would be done in a spreadsheet with all of the individual component masses and the driver’s mass.

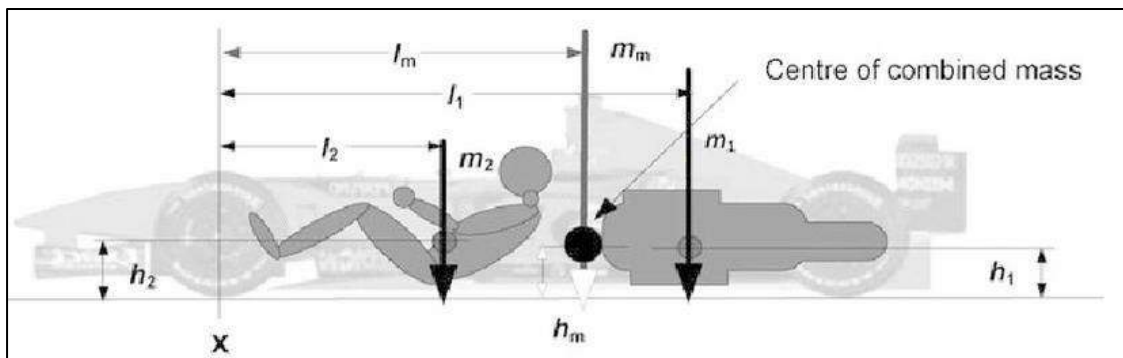


Figure 10 Centre of mass, lengths and heights (3).

$$m_m = \Sigma(m_1 + m_2 + \dots m_n) \tag{1}$$

$$l_m = \frac{\Sigma(m_1 l_1 + m_2 l_2 + \dots m_n l_n)}{m_m} \tag{2}$$

$$h_m = \frac{\Sigma(m_1 h_1 + m_2 h_2 + \dots m_n h_n)}{m_m} \tag{3}$$

When accelerating or decelerating (braking) there is a load transfer across the car to either the front or rear axle. Lowering the height of the centre of mass,  $h_m$  is very important when considering the load transfer across the car. Lowering,  $h_m$  will decrease the load transfer.

### 3.3 Longitudinal Load Transfer

In a simple static analysis by using Alembert’s principle of the car and only considering Newton’s second law of motion, the acceleration of the car will be limited by the centre of mass. This is due to the inertial reaction force that is acting through the centre of mass in the longitudinal direction.

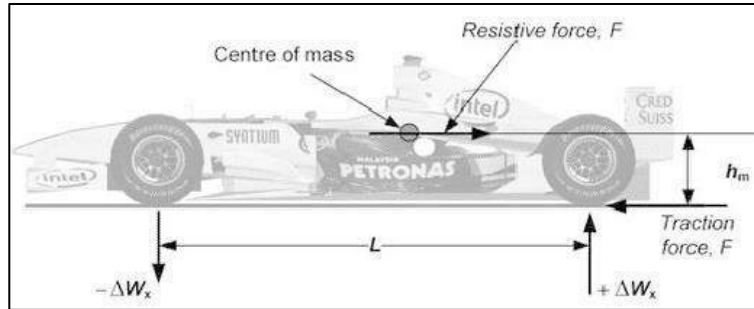


Figure 11 Linear acceleration and longitudinal load transfer (3).

This inertial reaction force is equal and opposite to the traction force which acts at road level. As these forces are acting at different heights an out-of-balance moment occurs which changes the static axle loads ( $W_F, W_R$ ). The magnitude of the change in  $W_x$  is the longitudinal load transfer. This load increases at the rear axle and decreases at the front axle as shown in figure 7. This is why with a very rapid acceleration, the front of the car rises and the rear lowers, which is called a squat (3).

Moments about front contact path, where  $h_m$  is the height of the centre of mass,  $F$  is the resistive force and  $L$  is the length between the axles as shown in figure 7.

$$F \times h_m = \Delta W_x \times L \tag{4}$$

$$\Delta W_x = \pm \frac{F h_m}{L} \tag{5}$$

Therefore, to minimise the longitudinal load transfer and increase the stability, the height of the centre of mass,  $h_m$  should be minimised.

### 3.4 Lateral load transfer

Lowering the height of the centre of mass also reduces the lateral load transfer when cornering. This in turn reduces roll and therefore less changes can be made to the camber angle. With this the team can maximise the tyre contact patch to give the car more traction off the line or when cornering.

Lateral load transfer when cornering, where  $T$  is the track width, and  $F$  is the centripetal force.

$$\Delta W_y = \pm \frac{F h_m}{T} \quad (6)$$

$$F = ma = m \left( \frac{v^2}{R} \right) \quad (7)$$

## 5 Concept Development

### 5.1 Louvre concept 1

For air cooling the high voltage system, a water-tight louvre can be used as an inlet and outlet for airflow to the engine bay. The louvre concept 1 is made of two sheets of 3mm sheet metal, that sandwich a hydrophobic mesh material to prevent water from passing into the engine bay, but allow air to pass. Any water that collects on the hydrophobic mesh material would be run off through water channels in the sheet metal as shown in figure 14.

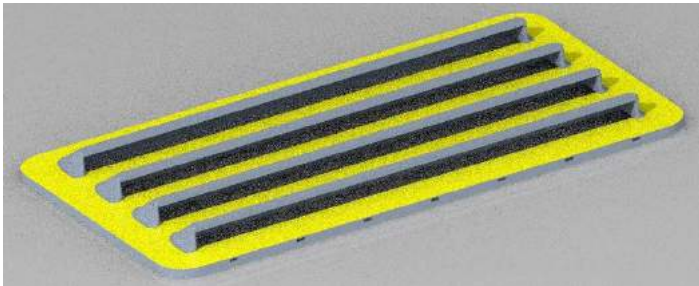


Figure 12 Louvre concept 1



Figure 13 Louvre exploded view.

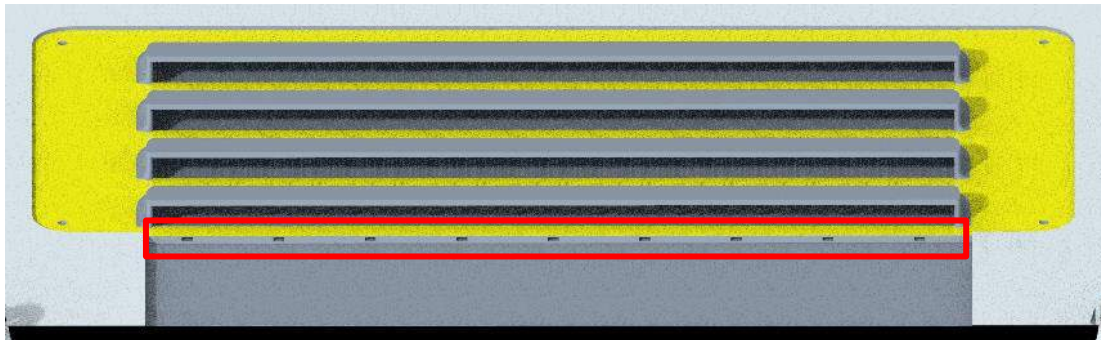


Figure 14 Louvre water drainage channels.

The sheet metal would be water jet cut, then the louvres would be punch formed. The issues with this concept is that it may not be water tight as a rubber seal has not been used and the size of the louvres is unrealistic to punch form.



Figure 15 Louvre on the engine bay cover.

The material selection for this type of louvre is shown in figure 16. Stainless steel was selected as the most suitable material for the louvre, mainly because of the price and the cold workability of the metal. It's also commonly used in many punch form applications. As the louvre is an external component of the car, corrosion resistance is also a very important aspect of it's design and stainless steel has very good properties for this.

Material	Grade	Tempers	Sheet size	Price	Cold workability	Elongation	Machineability	Corrosion resistance
Stainless steel	304		500mm x 500mm x 2mm	£40.03	Very good	30-40%		Very good
Mild steel	EN242	817M40T	500mm x 500mm x 2mm	£111.25	Good	20%	Very good	Poor
Aluminium	5251	H22	2500mm x 1250mm x 2mm	£117.42	Very good	14%	Average	Good

Figure 16 Louvre material selection.

## 5.2 Louvre concept 2

The manufacture of a punched form sheet metal louvre has certain calculations and conditions to determine the pitch and height of the openings on the louvre. The previous concept would have been impossible to do, unless the louvre vent was welded instead of punch formed which would add significant amount of lead time to the completion of the part.

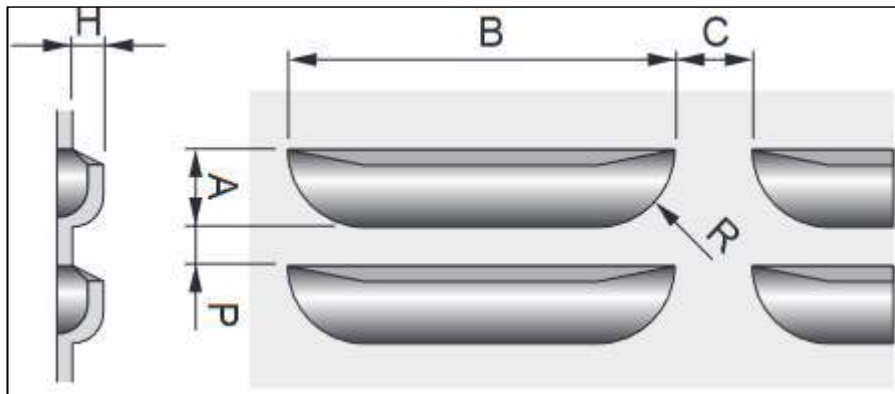


Figure 17 Punch form louvre dimensions.

$$\text{Pitch}(P) \geq 5\text{mm} \tag{8}$$

$$\text{Width}(A) \geq \text{Height}(H) \times 2 \tag{9}$$

$$\text{Height } (H) \leq \text{Material thickness} \times 3.5 \tag{10}$$

<i>Material thickness</i>	<i>Height (H)</i>	<i>Width (A)</i>	<i>Pitch (P)</i>
1mm	3.5mm	7mm	$\text{Pitch}(P) \geq 5\text{mm}$
2mm	7mm	14mm	$\text{Pitch}(P) \geq 5\text{mm}$
3mm	10.5mm	21mm	$\text{Pitch}(P) \geq 5\text{mm}$

The 2mm material thickness was selected for the design of the concept 2 louvre as given the available space on the engine bay for the louvre, these dimensions were the most suitable.

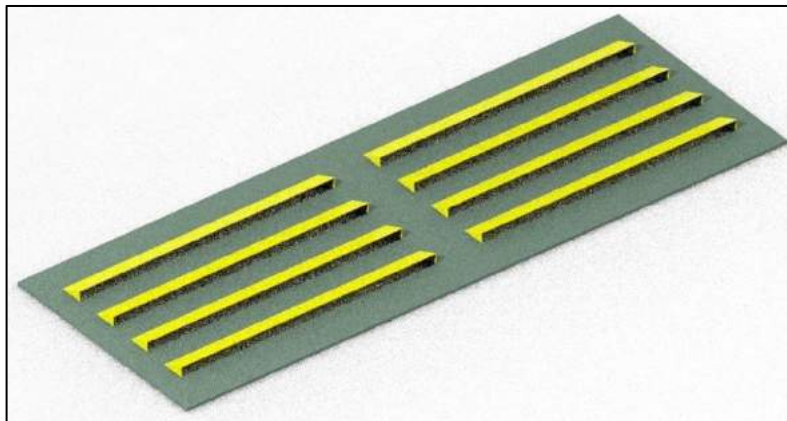


Figure 18 Louvre concept 2 (angle 1).

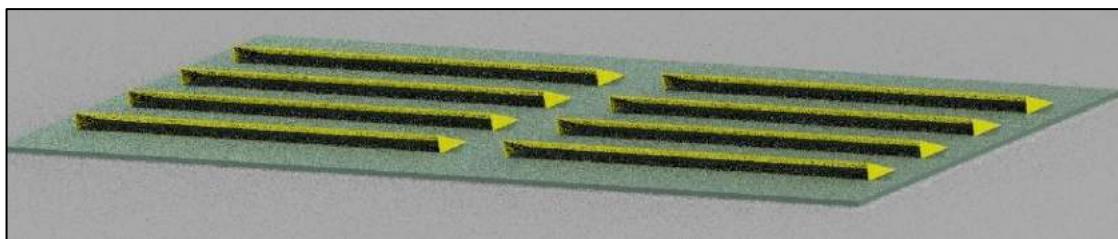


Figure 19 Louvre concept 2 (angle 2).

### 5.3 Louvre Concept 3

Concept 3 uses a carbon fibre louvre vent alternatively to stainless steel. The geometric tolerances are more difficult to control with the manufacture of the louvre however there are techniques to minimise inaccurate features. The carbon fibre louvre would be laid up on MDF with 5 layers of 193gsm 2x2 twill prepreg with alternative ply angles of 0° and 45°. With this many layers and the rigidity from the alternating ply angles, the louvre would be very rigid.

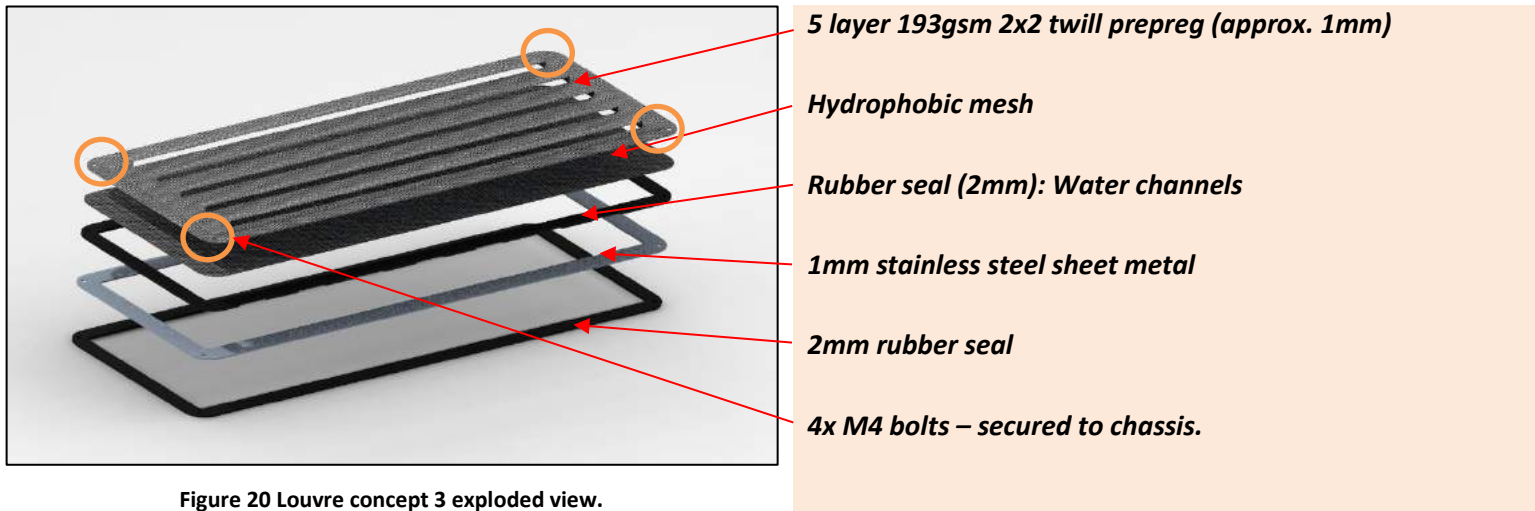


Figure 20 Louvre concept 3 exploded view.

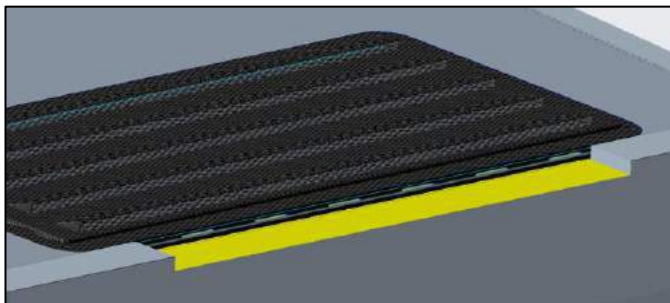


Figure 21 Louvre assembled to engine bay cover.



Figure 22 Hydrophobic mesh materials.

The hydrophobic mesh material shown in figure 19 allows air to pass but not water. The idea is that any water that passes through the louvre would collect on the hydrophobic mesh and be run off through water channels in the rubber seal off the rear of the chassis. The two rubber seals prevent any leaks into the engine bay. To maintain high geometrical tolerances to prevent any leaks, the engine bay cover would be machined after layup, and the outer edges of the louvre would also be machined to the correct size.

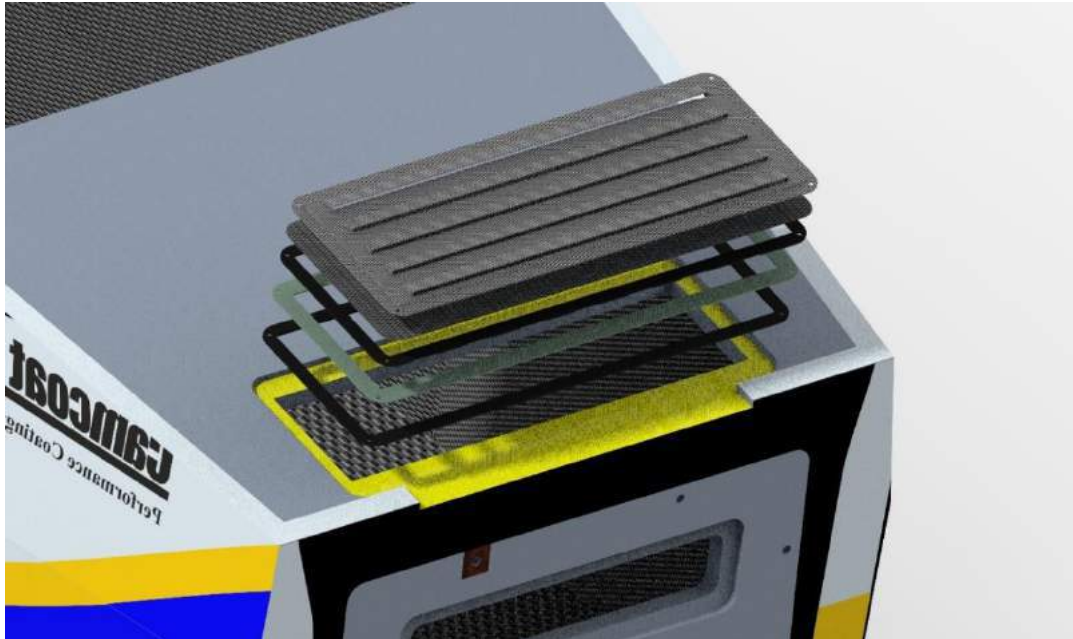
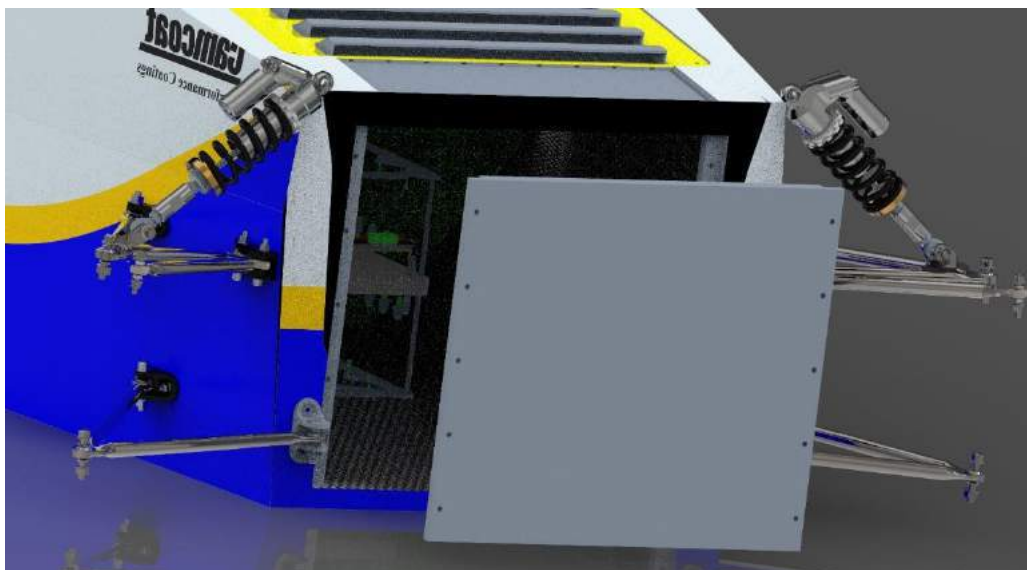


Figure 23 Louvre on engine bay (exploded view).

#### 5.4 Removable panel concept 1

The suspension mounts have been moved closer to the outermost edge of the chassis to allow more space for the battery and the removable panel. The removable panel concept seen below is constructed of 15mm Rohacell and a laminated 4mm Aluminium, anti-intrusion plate, sandwiched between 10 layers of prepreg in total. This layup is to comply with the SES on the protection of the accumulator as mentioned previously. The removable panel would be attached to the chassis with ten, 8mm diameter bolts.



The issue with this concept is with the structural integrity of the panel. The sharp corners are likely to obtain cracks from the loads from the suspension. Making this concept water-tight would also be very

difficult. No rubber seal could be used across the top section or the bottom, therefore water is likely to pass into the engine bay.

### 5.5 Removable panel concept 2

Concept 2 has been developed significantly with a full outer lap joint. Again, this panel is constructed of the layup mentioned in the previous concept. The panel is attached to the chassis with six, 8mm diameter bolts and a 2mm rubber seal is used to prevent water leaks into the engine bay. Another louvre vent, with the same construction as louvre concept 3 is used to provide additional air flow to the engine bay. The louvre is placed at the top of the engine bay for safety reasons for the protection of the battery, as the anti-intrusion plate goes below this louvre.

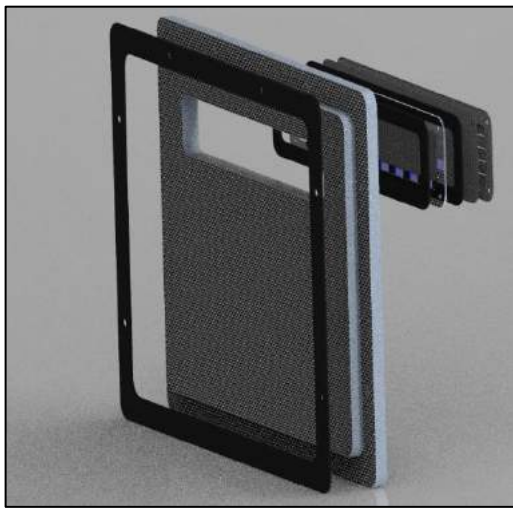


Figure 24 Removable panel concept 2 (1st angle).



Figure 25 Removable panel concept 2 (2nd angle).

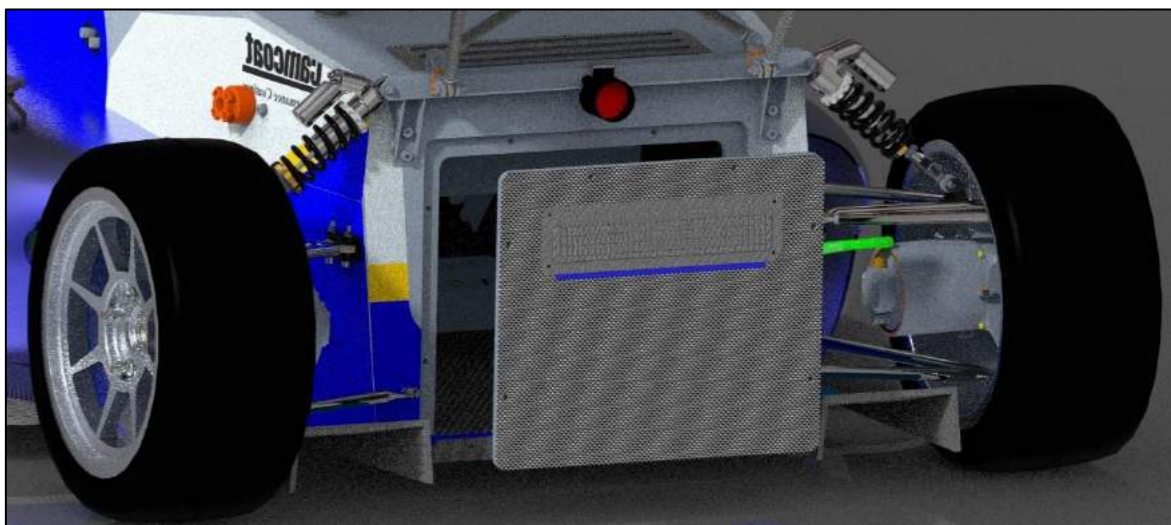


Figure 26 Rear bulkhead removed from chassis.

Any water that passes through the louvre can run off through the drafted angle shown in figure 27. The non-detachable rear bulkhead structure is machined prior to the layup to create the lap joint. The lap on the structure is laid up with prepreg before it is placed into the chassis mould, in order to secure tufnol inserts in place.

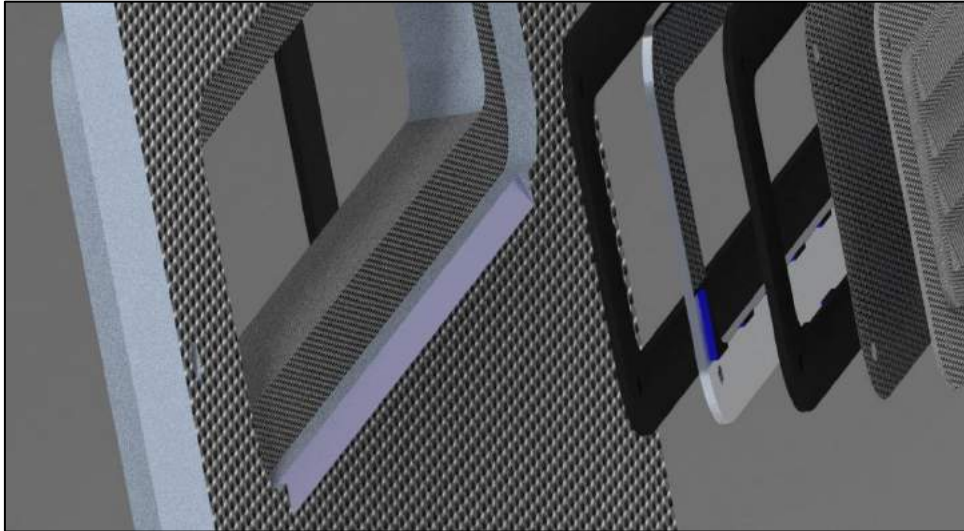


Figure 27 Drafted angle to allow water to escape the louvre.

## 5.6 Engine bay cover

The engine bay cover will be attached in the third cure of the chassis, when the firewall is also cured in its position on the chassis. The cover will be secure in place using Permabond as shown in the figure below. The Rohacell sections on the side are machined with a lap so that the engine bay cover sits flush with the rest of the chassis.

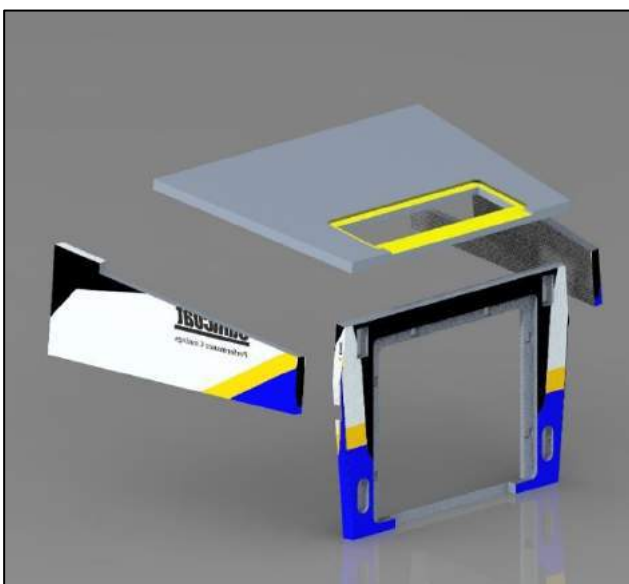


Figure 28 Rohacell core sections of chassis.

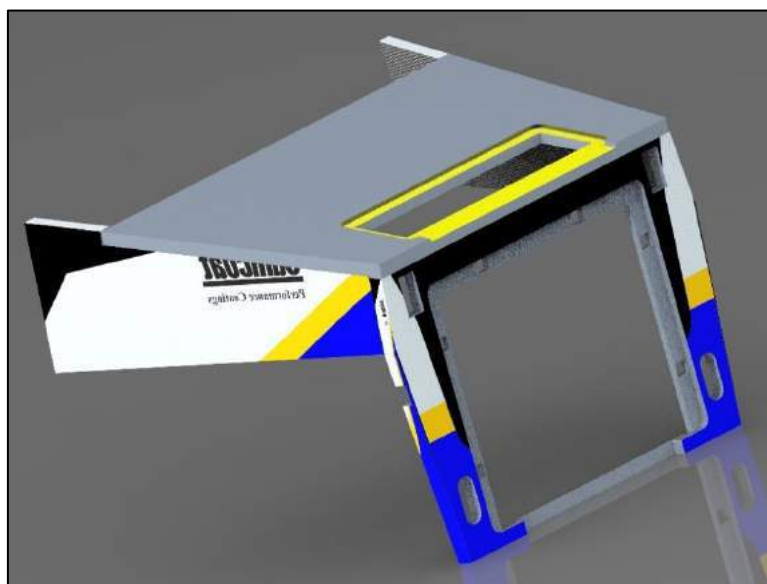


Figure 29 Assembled rohacell cores.

## 6 SES

With the changes to the chassis, there are a few minor changes to the SES. One is with the attachment for the supports for the main hoop to the engine bay cover. The plan is to copy the ULM012 attachment dimensions as these still comply and pass the 2021 SES. The same prepreg that was used for the ULM015 SES was no longer available to the team due to the lead time. This prepreg was supplied by Amicon, and it was 245 gsm 2x2 twill. Alternatively, the team decided to impregnate 293gsm, 6k carbon fibre with the help of SHD with a resin the MTC510 resin, which has similar properties and cure cycles to the Amicon EY440. With this change, new test panels were constructed only for the side impact structure, to prove that the SHD prepreg was just as strong or stronger than the Amicon prepreg.

MTC510 epoxy was selected as it has very similar properties to the Amicon prepreg. The data sheet for this prepreg can be found in Appendix B. It has a tensile and compressive strength of 645Mpa and 615Mpa respectively and a cure cycle between 80°C to 120°C which is ideal for the application. It also has very good aesthetic qualities with an excellent surface finish.



Figure 30 Instron three point bend test.

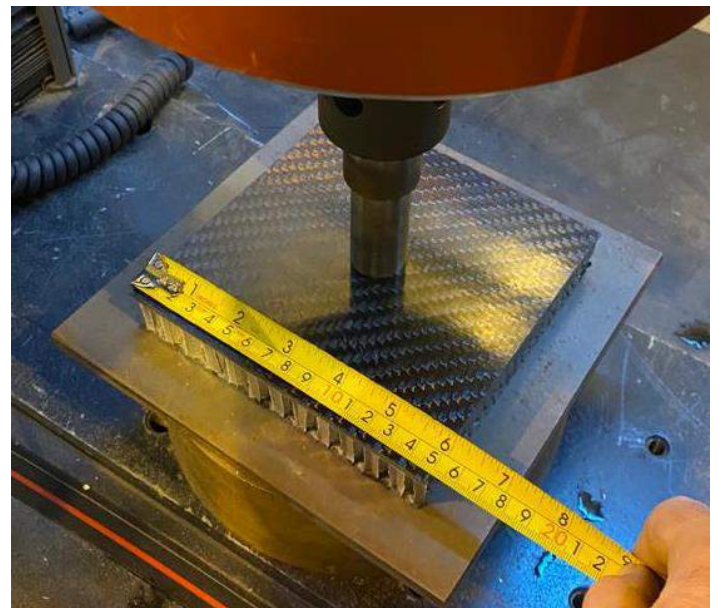


Figure 31 Instron shear test.



**Figure 32 Instron harness pull out test.**

Three test panels were manufactured and a three point bend test, shear test and harness pull out test was performed on the Instron machine in the brodie. The Instron has pre-defined set ups for these tests. The graphs below and the data for these graphs are inputted in the SES. For the bend test and shear test, the integral under the graph (Work = force x displacement) determines the amount of energy that the panel can absorb in the first peak. The amount of energy the panel can absorb determines whether the panel can pass the SES or not. For the harness pull out test, this is used to just determine the maximum out of force the panel can withstand in pull out failure. All of the tests passed the SES.

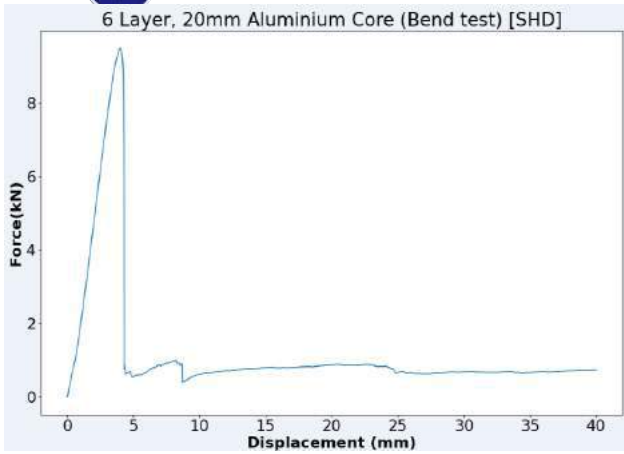


Figure 33 Force-displacement graph (Bend test).

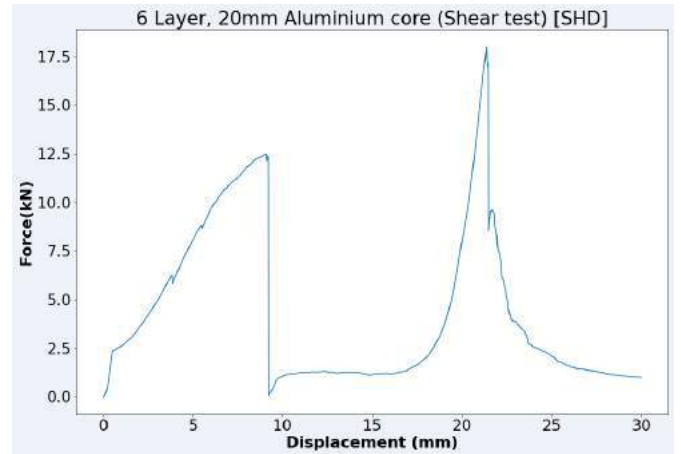


Figure 34 Force-displacement graph (Shear test).

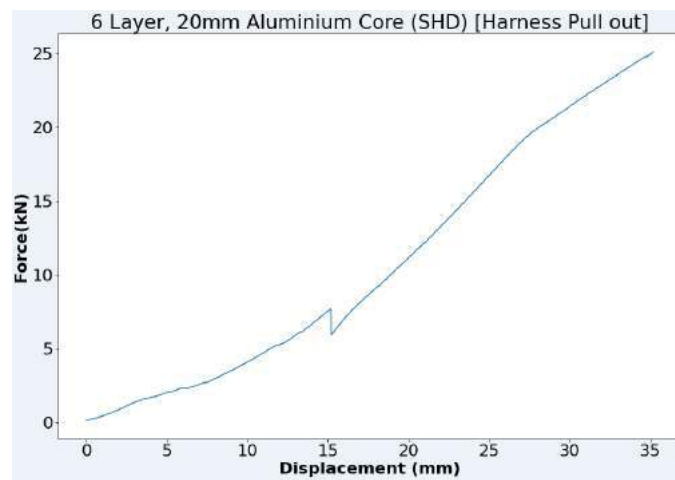


Figure 35 Force displacement (Harness pull out test).

## 7 Manufacturing process

### 7.1 Chassis layup construction

The layup breakdown can be seen in the figures below. Each one of the constructions have been tested to be compliant with the SES. The main changes from the prior SES construction is with the rear bulkhead and the engine bay cover. For each one of the panels, plywood templates were laser cut for the cutting out of the prepreg.

ULM016 Chassis Composition			
Chassis section	Name	Description	Ply Orientation Schedule
S1	Front Bulkhead	Composite 15mm, Rohacell Core and Laminated 4mm Al plate	(0,45,0,45,0,45) Al plate (45,0,45,0)
S2	Front Bulkhead support	4 Layer, 20mm Rohacell Core	(0,45,0,45) Core (45,0,45,0)
S3	Front Hoop Brace	6 Layer, 20mm Rohacell Core	(0,45,0,45,0,45) Core (45,0,45,0,45,0)
S4	Side Impact Structure (Upper and Diagonal)	6 Layer, 20mm Aluminium Core	(0,45,0,45,0,45) Core (45,0,45,0,45,0)
S5	Side Impact Structure Floor (Lower)	6 Layer, 20mm Aluminium Core	(0,45,0,45,0,45) Core (45,0,45,0,45,0)
S6	Chassis Wall Above SIS	2 Layer, 20mm Aluminium Core	(0,45) Core (45,0)
S7	Chassis Floor Rear of SIS Floor	4 Layer, 20mm Rohacell Core	(0,45,0,45) Core (45,0,45,0)
S8	Chassis Wall Rear of SIS Floor	4 Layer, 20mm Aluminium Core	(0,45,0,45) Core (45,0,45,0)
S9	Engine bay cover	4 Layer, 20mm Rohacell Core	(0,45,0,45) Core (45,0,45,0)
S10	Firewall	4 Layer Flame Retardant, 15mm Rohacell Core.	(0,45,0,45) Core (45,0,45,0)
S11	Rear Bulkhead	Composite 15mm, Rohacell Core and Laminated 4mm Al plate	(0,45,0,45,0,45) Al plate (45,0,45,0)

Note: All Piles are of the same prepreg carbon fibre MTC510 as included in the Additional Info (Prepreg) tab. The curing of skins will be performed as per the 16 hour curing profile recommended by the manufacturer in the (Epoxy Data) tab.

Figure 36 ULM016 Chassis Composition.

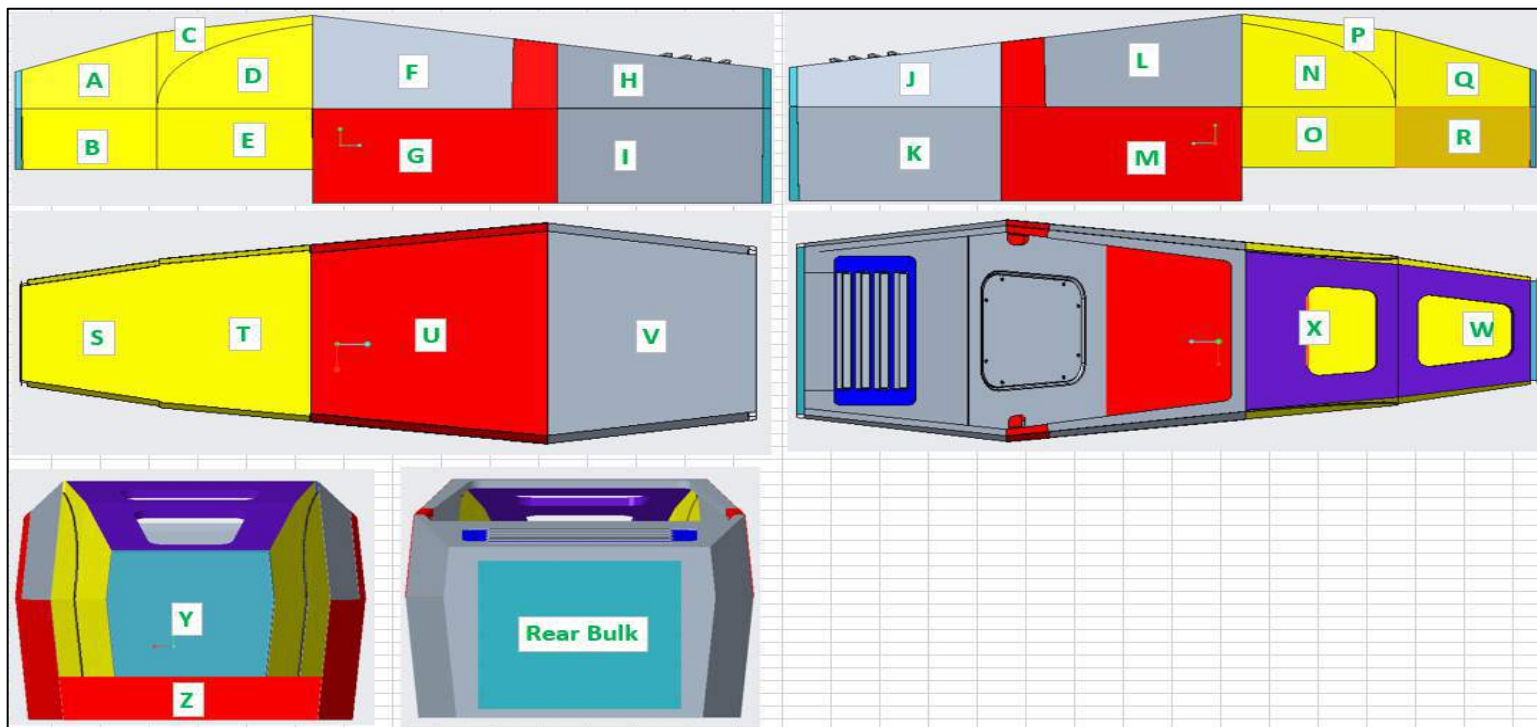


Figure 37 Panel breakdown labels.

## 7.2 Layup

### 7.2.1 Mould prep

**Steps:**

1. Hoover the inside of the mould
2. Push wax into all of the corners of the chassis to create the rounded corners
3. Seal all the sharp edges → use rubber and flash tape
4. Hoover the mould again
5. Mould cleaner
6. Mould release agent



Figure 38 Rounder tool for wax.

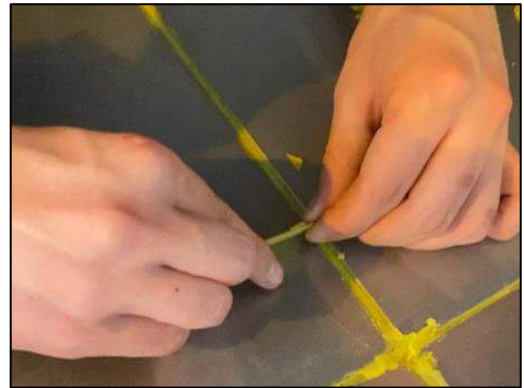


Figure 39 Putting wax in all the edges.



Figure 40 Gum tape around sharp outer edges.



Figure 41 Prepped mould.



Figure 42 Rubber and flash tape to cover bolts.

### 7.2.2 Prepreg cut out and layup

Each panel of the chassis has a plywood template, and each layer alternates at a ply angle of  $0^\circ$  and  $45^\circ$ . The template has to be orientated correctly to cut out the correct ply angle as demonstrated in figure 43. The checklist for the prepreg for the chassis can be found in appendix C. With the templates, they have overlaps with other sections of the chassis of around 2cm to ensure good consolidation of the prepreg layers. For any corners it's important that you don't overlap the prepreg twice. A demonstration of this can be seen in figure 44. If you overlap the corners twice, this can lead to bridging with reduces the tolerance of your part and also reduces the strength in these corners. When doing the layup, it is also much easier to push a single overlap into the corners, as there is much less friction between the surfaces.

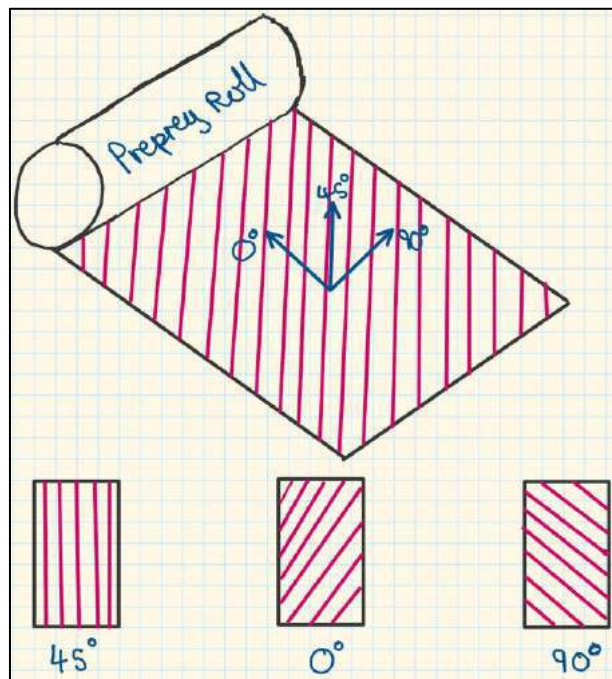


Figure 43 Ply angles on prepreg roll.

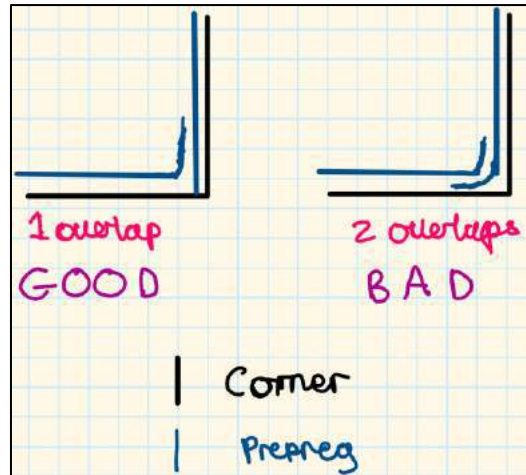


Figure 44 Overlapping of prepreg in corners.

Figure 45 demonstrates how the chassis should be laid up. The opposite side of the blue backing film is the surface needed on the outside of the chassis as it has the best finish. The blue backing film is left on to prevent any contamination of prepreg when climbing in and out of the chassis. The bottom layers were done first, then the side and then the top. It was done in this order to keep track of which layers have gone in.



Figure 45 1st layer complete.

Once all the layers have been laid up, peel ply is added to all of the surfaces of the prepreg on the inside of the mould. Peel ply helps to create an abrasive surface so that the core materials have something to grip to, making it more difficult for them to move around during the cure.



Figure 46 Peel ply secured with flash tape.

### 7.2.3 Inserts

For attachment of components to the chassis, due to the low compressive strength and limited grip strength of Rohacell and aluminium honeycomb, inserts must be used to handle the weight and dynamic forces of the components. Tufnol is a high compressive strength material that is laid within the second layup of the chassis. Where there is a tufnol inserts, the core materials are machined or water jet cut to include a slot for the inserts. Plywood templates mark out where these inserts are positioned in the layup and then the chassis can be post drilled in these insert locations. A free body diagram of the forces acting on the insert is shown.

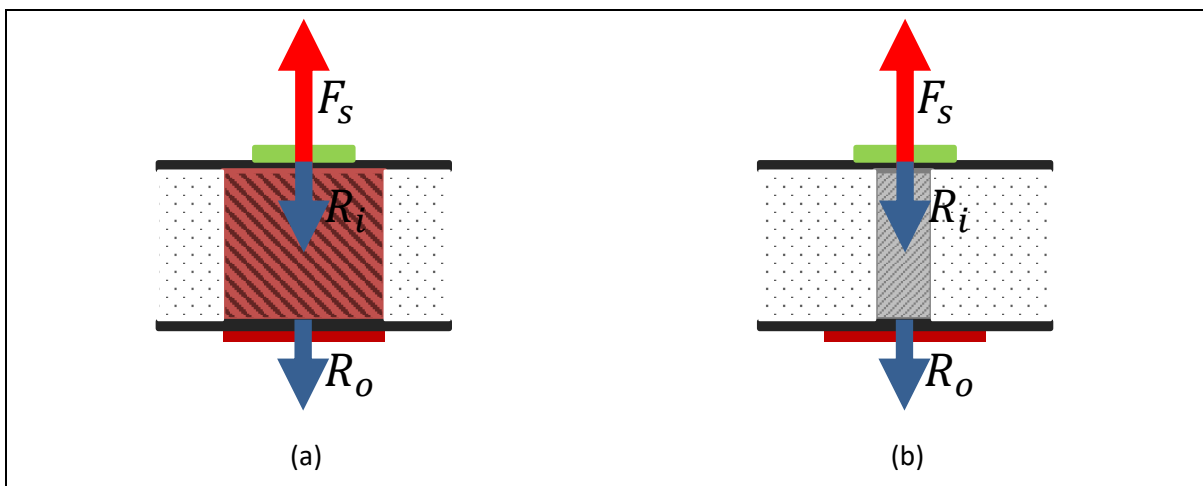


Figure 47 Free body diagram tufnol insert

$$\begin{aligned}
 R_i &= t_i \times P_{insert} \times \sigma_s \\
 R_o &= t_o \times P_{plate} \times \sigma_s \\
 F_s &= R_i + R_o
 \end{aligned}
 \tag{50}$$

$$F_s \propto P_{insert}$$

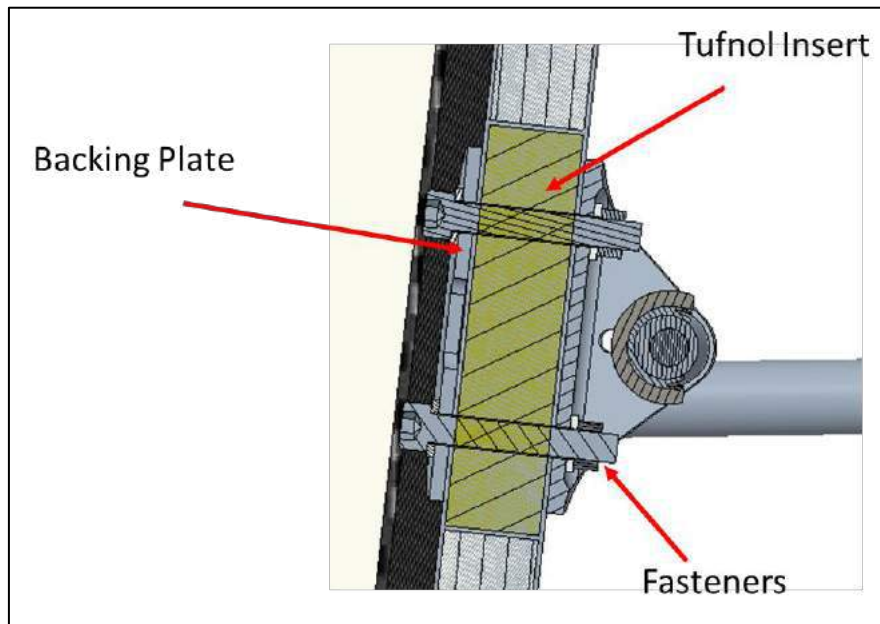
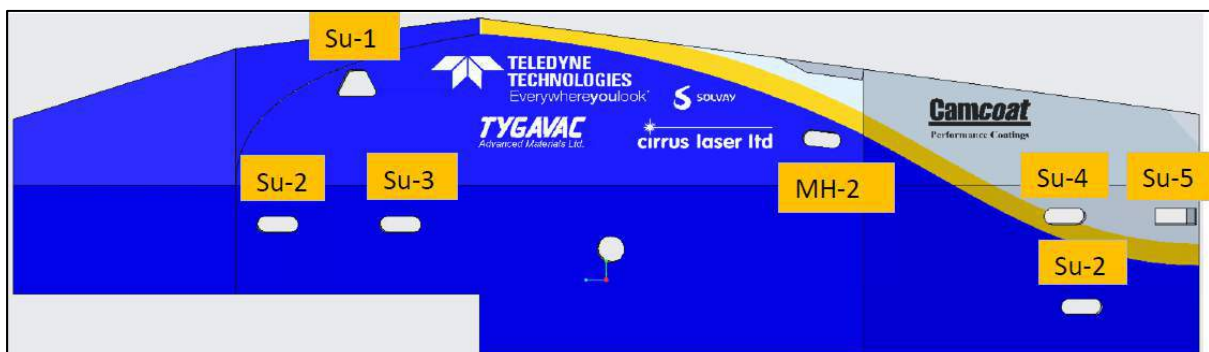
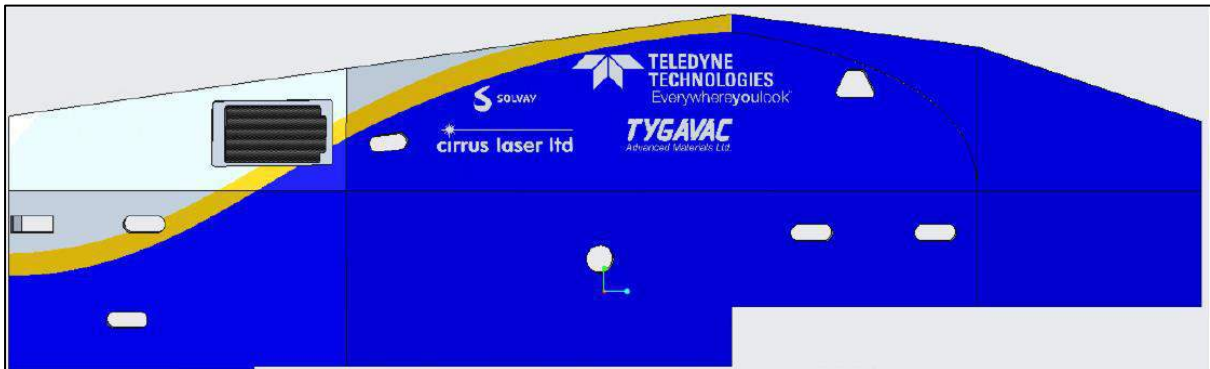
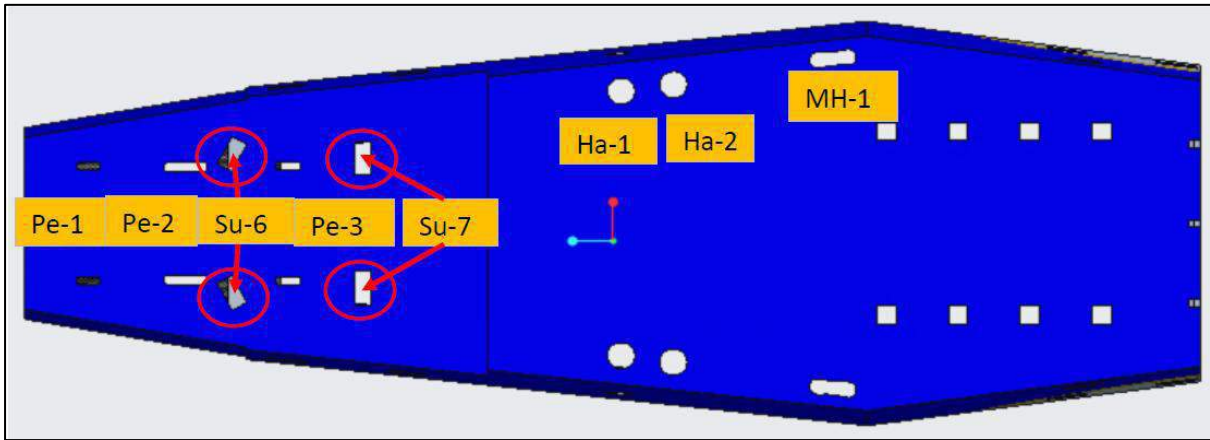
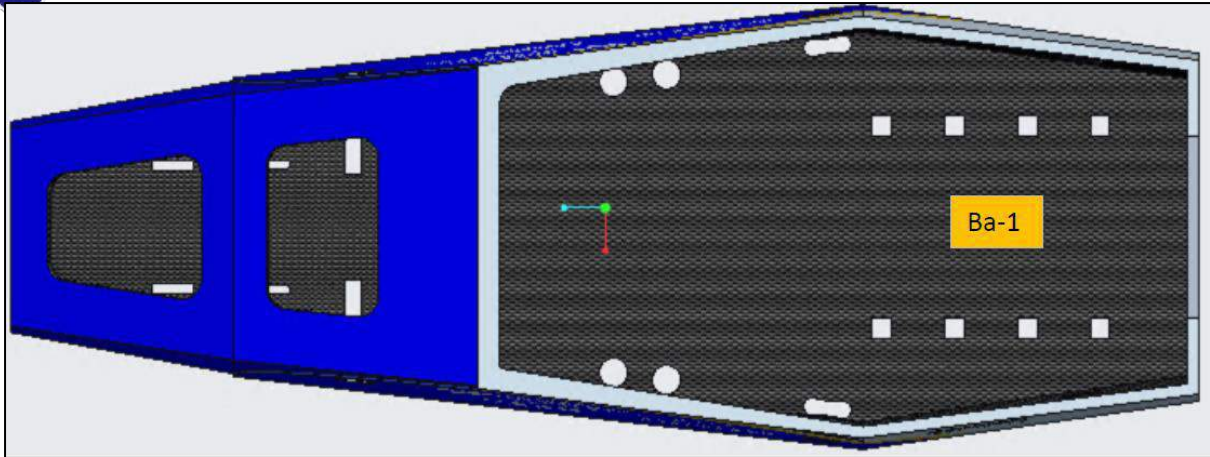


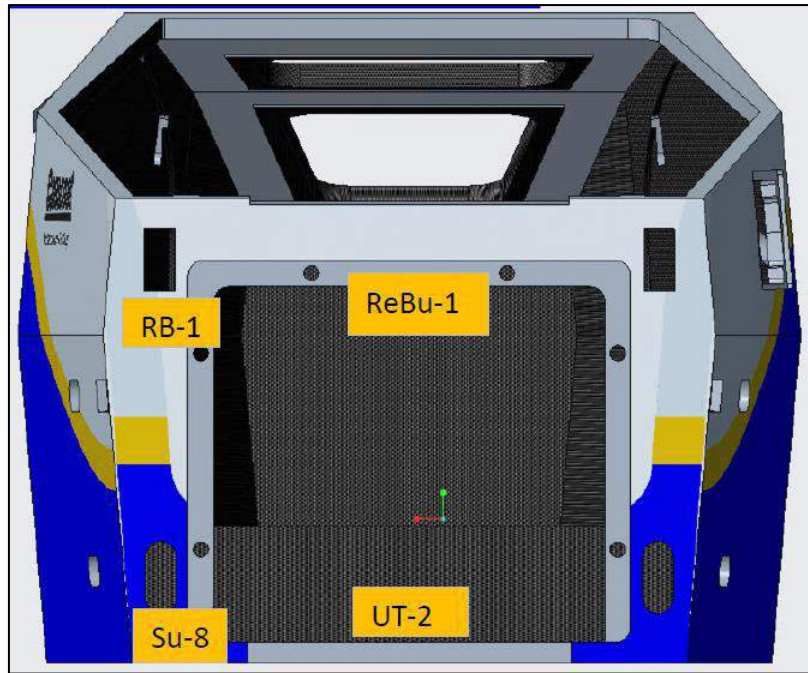
Figure 48 Cross section of suspension mount.

Inserts	Quantity	Done?	Key
Su-1-L-R	2		Su - suspension
Su-2-L-R	2		Pe - pedal box
Su-3-L-R	2		Ha - Harness
Su-4-L-R	2		MH - main hoop
Su-5-L-R	2		Ba - battery
Su-6-L-R	2		RB - Rear brace
Su-7-L-R	2		Ra - radiator
Su-8-L-R	2		UT - Undertray
Pe-1-L-R	2		L-R: Left and Right
Pe-2-L-R	2		ReBu-Rear bulkhead
Pe-3-L-R	2		
Ha-1-L-R	2		
Ha-2-L-R	2		
MH-1-L-R	2		
MH-2-L-R	2		
Ba-1-L-R	8		
RB-1-L-R	2		
Ra-1-L-R	2		
UT-1-L-R	2		
UT-2	1		
ReBu-1	6		

Figure 49 Insert location list.

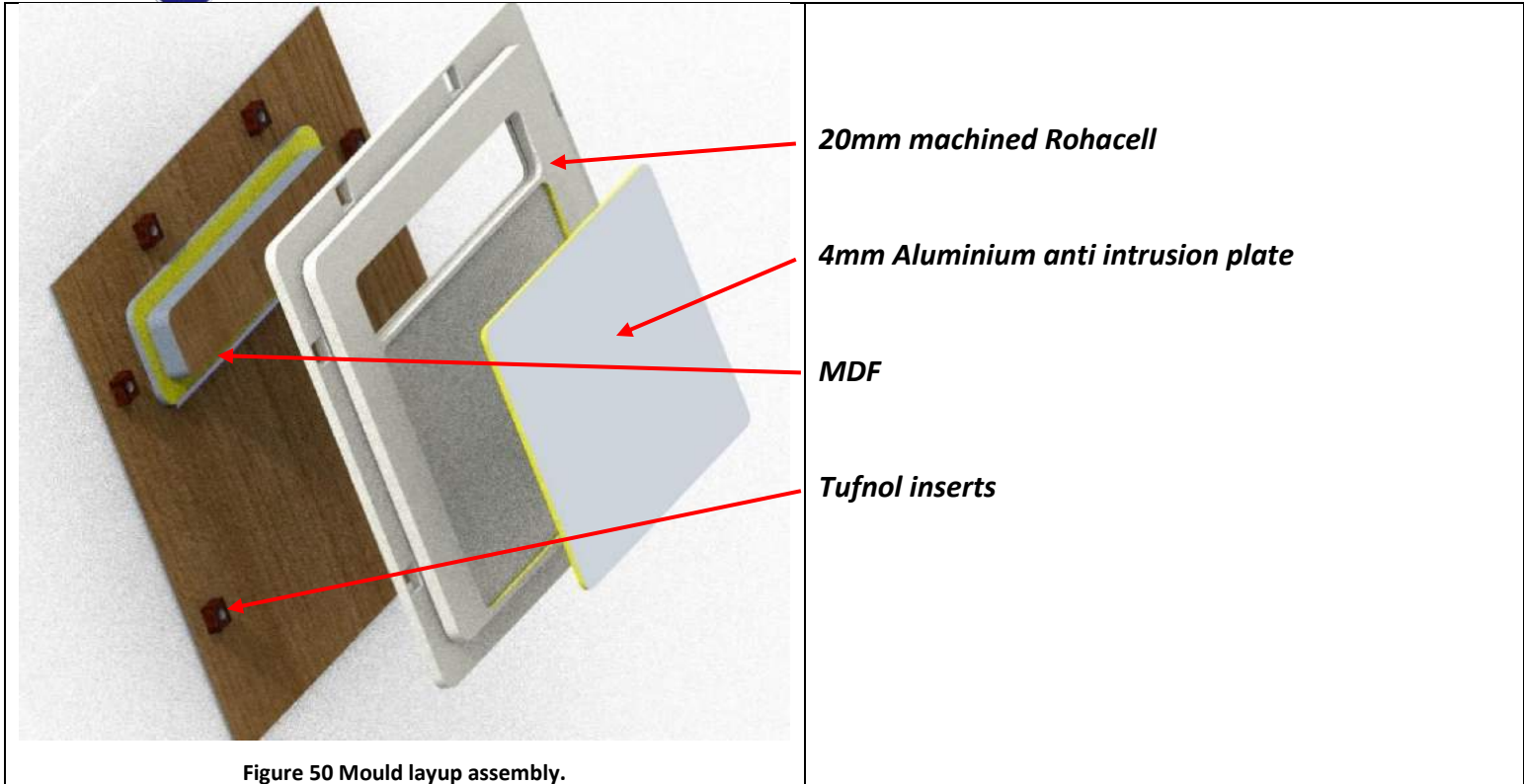






### 7.3 Rear bulkhead

The rear bulkhead uses an MDF mould. There is an extra step for the mould prep at the start compared to the chassis. Before the mould cleaner and mould release agent is applied, the MDF must be sealed using a mould sealer. This is to prevent the cleaner and release agent from soaking into the mould. The Rohacell and the MDF board can be machined on the CNC.



The 1st 4 layers would be laid up onto this MDF board and cured in the autoclave. In the second cure, the rohacell, inserts and the next 4 layers of carbon fibre can be laid up and then cured again in the autoclave. The MDF mould has been made larger than the actual part so that the rear bulkhead can be machined to the correct size after the second cure. This is to maintain a high level of accuracy with the dimensions so that the rear bulkhead is water tight.

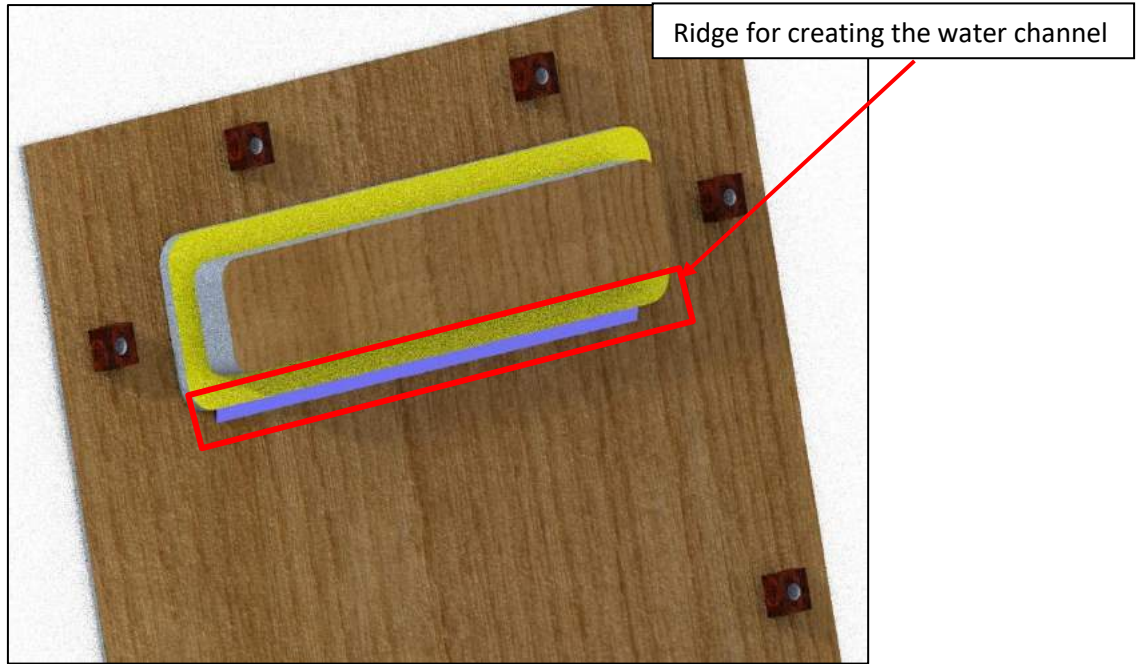


Figure 51 Machined MDF rear bulkhead mould.

## 7.4 Louvre

The louvre will be laid up on an MDF mould. The mould has been made larger than the part so that it can be post processed to the correct size, so that the fit between the louvre and the engine bay is water tight. Figure 52 demonstrates this, where that hooded vent component would need to be post processed to the correct size. The louvre will be made of 5 layers of 293gsm 2x2 twill with alternating ply angles of 0° and 45°. Draft angles of 10° have been included on the louvre mould to make it easier to remove carbon fibre part without damaging the mould.



Figure 52 Louvre MDF mould.



Figure 53 Louvre laid up on MDF.

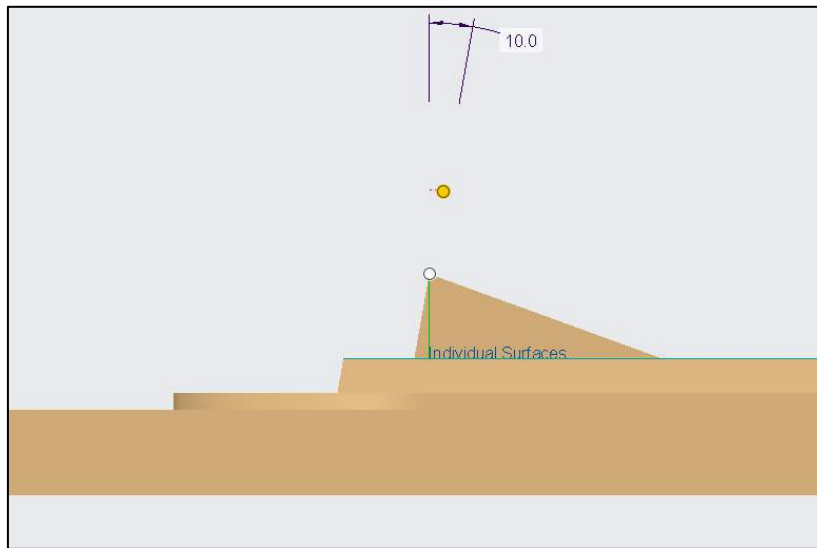


Figure 54 Draft angles on Louvre mould.



Figure 55 Hooded vent to be post processed to correct size.

Once the 5 layers have been cured in the autoclave, the gaps of the louvre can then be cut out using a rotary blade. The hydrophobic mesh can be secured in place using a glue gun as shown in figure 54.



**Figure 56 Mesh superglued onto cured carbon fibre,**

# **SCHOOL OF ENGINEERING FORMULA STUDENT**

**Design Methodology**

**ULM016 Battery cooling.**

**Christopher Cooper  
Mechanical Engineering**



## Summary

This report details the design process of ULM016's battery cooling system and calculations. In its current progress, the concepts are at the very beginning of the design process. Modelling battery temperature without having the experimental temperature data of the cells is very difficult to do because there are many different fluctuating variables based upon changing parameters of the battery; for example, temperature, internal resistance, state of charge(SOC), state of health(SOH), voltage, current and resistance. Many of these parameters are modelled as functions of temperature which makes it very difficult to accurately estimate the values. A more accurate method is to model an equivalent circuit of the battery using a Simulink package called Simscape Electrical. The plan for semester two is to develop one of these models for the battery. For the current progress of the battery cooling, the model has been simplified with many different assumptions and estimations to obtain a general idea of the cooling requirements for our 439.9V battery. The batteries must be air cooled according to the rules and the battery must also have a type of heat sink material to pull some of the heat away from the cells.

## 2 Design Brief

### 2.1 Introduction

With the now closed engine bay, it is very important to have forced convection for the high voltage system by using fans and also by allowing air to pass into the engine bay from the momentum of the air passing over the car. For the battery the cells have an optimum performance temperature range. If the cells are outside of this temperature range the battery parameters can be affected. More specifically, the state of charge (SOC) and the state of health (SOH) will deteriorate at a greater rate. The state of charge is the equivalent of the fuel gauge on an internal combustion car and the state of health is the ratio between the maximum battery charge of a fresh battery compared to its aged rated capacity.

While it is important to allow air to pass through the engine bay, it is also important to prevent water contacting the high voltage system. Even if it does not rain at the competition, the car still must pass a rain test.

### 2.2 Background information

#### 2.2.1 Transition from IC to EV

This is the first year of the University of Liverpool's transition from internal combustion (IC) engines to an electric powertrain. Concepts for cooling are based upon the face value of what can be seen in assembly videos of formula student electric vehicles and what is done in industry with electric road vehicles. Most electric road vehicles use a coolant through pipes/plates however there are some high voltage systems that are air cooled such as in Nissan Leaf. According to Tesla, air cooling is considered less safe than liquid cooling (1), therefore formula student rules might eventually transition to liquid cooling. Air cooling could especially be dangerous in hot climate countries.

#### 2.2.2 Relevant FS rules

The main rules for cooling are that the battery must be air cooled and the cells must also not exceed a battery temperature of 60°C [T11.7.7]. The rules also dictate that the TSAC (tractive system accumulator container) is allowed openings if they are used for cooling [EV5.5.14]. The fans are also allowed to be contained within the TSAC even though they are part of the low voltage system (LVS)[EV5.4.3].

## 2.3 Aims and Objectives

The aim of this work package is to determine the amount of air flow required by the fans and also the material to be used as a heat sink for the cells to maintain the battery at an optimal operating temperature.

Objectives of this work package:

- To research and identify the best methods to model battery parameters to determine the battery temperature over the time of the endurance event.
- To complete simplified thermal model/hand calculations for modelling battery temperature.
- To create a Simscape electrical model of the battery and determine, SOC, SOH, battery temperature and discharge characteristics.
- To determine the amount of heat energy to be dissipated then determine number of fans and the flow rate of the fans to maintain the battery at an optimal temperature.
- To determine the best heat sink material to maintain the batteries SOH.

### 3 Engineering Science

#### Nomenclature

##### List of symbols

$F_{air}$	Drag force [N]	$P_w$	Power at the wheel [W]
$\rho_{air}$	Density [ $kgm^{-3}$ ]	$P_I$	Power at the inverter [W]
$A_f$	Frontal area [ $m^2$ ]	$P_m$	Power at the motors [W]
$C_D$	Drag coefficient [No unit]	$P_b$	Power at the battery [W]
$V$	Velocity [ $ms^{-1}$ ]	$m_{pcm}$	Mass of the PCM [kg]
$V_{air}$	Velocity of air [ $ms^{-1}$ ]	$c_{p,pcm}$	PCM specific heat capacity [J/kgK]
$F_r$	Rolling resistance [N]	$h_{pcm}$	Heat transfer coefficient (PCM) [ $Wm^{-2}k^{-1}$ ]
$\mu_r$	Coefficient of friction [No unit]	$A_b$	Area around all modules [ $m^2$ ]
$M$	Mass [kg]	$T_b$	Temperature of the battery [K] or [ $^{\circ}C$ ]
$g$	Gravity [ $ms^{-2}$ ]	$T_{pcm}$	Temperature of the PCM [K] or [ $^{\circ}C$ ]
$\alpha$	Angle of gradient [ $^{\circ}$ ]	$h_{ext}$	Heat transfer coefficient (air) [ $Wm^{-2}k^{-1}$ ]
$F_a$	Force due to acceleration [N]	$A_{ext}$	Area around battery casing [ $m^2$ ]
$\frac{dV}{dt}$	Acceleration [ $ms^{-2}$ ]	$T_{ext}$	Ambient temperature around battery [K] or [ $^{\circ}C$ ]
$F_t$	Tractive force [N]	$L_s$	Latent heat of fusion [kJ/kg]
$F_g$	Force due to gradient [N]	$\gamma$	Dimensionless inclination
$t$	Time [s]	$\Delta T$	Temperature interval of phase transition [K] or [ $^{\circ}C$ ]
$T$	Ambient temperature of PCM [K] or [ $^{\circ}C$ ]	$P_{loss}$	Heat energy generated by discharge [W]
$R_{th}$	Thermal resistance of cell [ $^{\circ}C/W$ ]	$t_c$	Thermal time constant [s]

#### 3.1 Battery capacity requirement calculations

The battery capacity requirements can be determined from speed-time data from a formula student vehicle around the endurance track. As a team, this data has never been logged for any of our previous cars and therefore alternatively this data has been estimated based upon the graph of a Formula Student Germany electric vehicle team as shown in figure 1. In the future, this data should be obtained more accurately either by developing our own track simulation tool or by using software such as Optimum Lap or simulations that can be found on GitHub. However, the difficulty with running simulations from GitHub is that the track dimensions are unknown and therefore Optimum Lap is the most suitable. The data obtained from these calculations have then been used for the

battery cooling requirement calculations. These calculations are simplified and the car is modelled as a point mass.

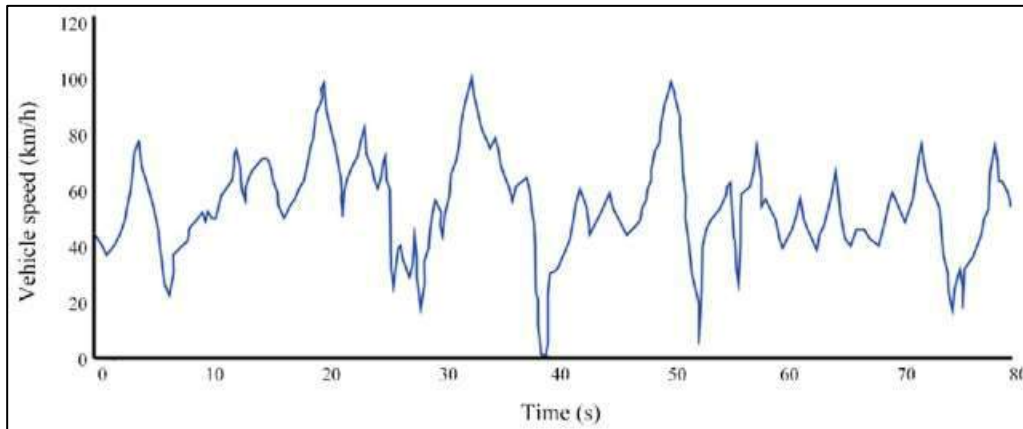


Figure 1 Speed(km/h) vs Time(s) graph for a single lap from Formula Student Germany (2).

### 3.1.1 Explanation of python code

With the estimated speed-time data, when you differentiate speed-time with respect to time you obtain the acceleration-time data. When the vehicle is decelerating the acceleration is negative and no power is being used from the battery as only the brakes are being applied and regenerative braking is not considered.

Parameter	Value
Density of air (kg/m <sup>3</sup> )	1.225
Frontal area (m <sup>2</sup> )	1.218
Rolling resistance coefficient	0.01
Mass of car	320
Speed of air	0
Coefficient of friction of track	0.7
Motor efficiency	0.75
Drag coefficient	1.04
Motor controller efficiency	0.98

Figure 2 Parameters used for the calculations.

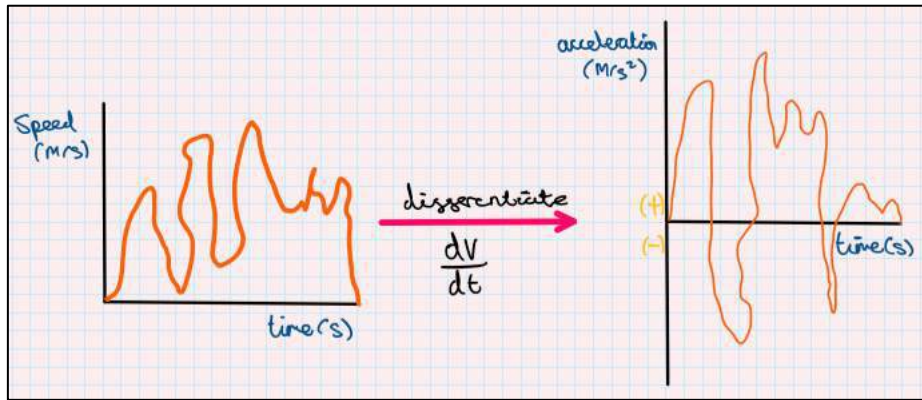


Figure 3 Differentiation of speed-time data.

The vehicle is modelled as a point mass and the force parameters considered are drag resistance,  $F_{air}$ , rolling resistance,  $F_r$ , gradient resistance,  $F_g$  and the acceleration force required to reach a certain acceleration (Newtons second law),  $F_a$ .

$$F_{air} = \frac{\rho_{air} A_f C_D (V + V_{air})^2}{2} \quad (1)$$

For the velocity of air,  $V_{air}$ , this is assumed to be zero.

$$F_r = \mu_r M g \cos(\alpha) \quad (2)$$

The gradient of the track,  $\alpha$ , is assumed to be 0 in these calculations, and therefore  $\cos(0)$  is just equal to 1 and the force from the gradient of the track is assumed to be zero.

$$F_g = M g \sin(\alpha) \quad (3)$$

$$F_a = M \frac{dV}{dt} \quad (4)$$

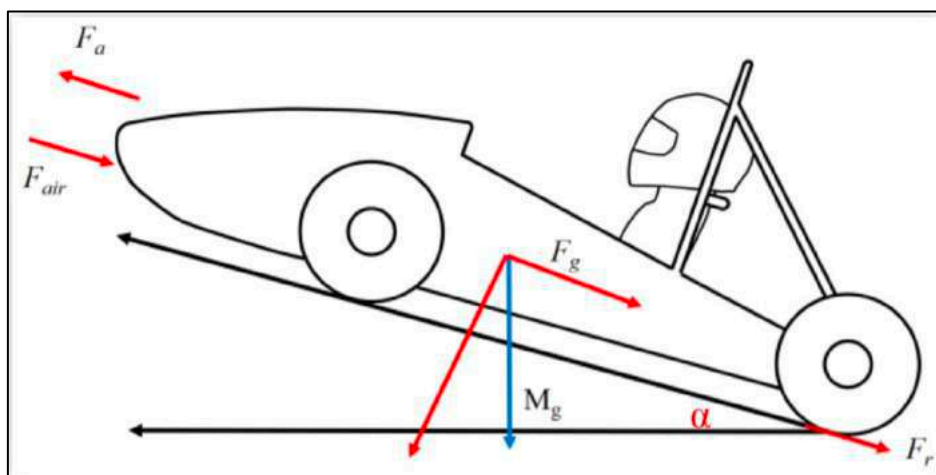


Figure 4 Free body diagram of forces (3).

Resolving for the forces from the free body diagram for the total tractive force,  $F_t$ , acting on the car which is defined as the force required to reach a desired acceleration, can be seen in equation 5.

$$F_t = M \frac{dV}{dt} + (F_g + F_r + F_{air}) \quad (5)$$

As mentioned before, when the acceleration is negative, no force (power) is being used by the battery. Therefore, for values of the tractive force that are less than zero, are converted to zero in the array of values. The tractive force calculated is the force required at wheels of the vehicle and the power requirement at the wheels,  $P_w$ , is calculated using equation 6.

$$P_w = F_t \times V \quad (6)$$

Due to efficiency losses, the power requirement at the wheels will be less than the power requirement at the accumulator (battery) as demonstrated by figure 4.

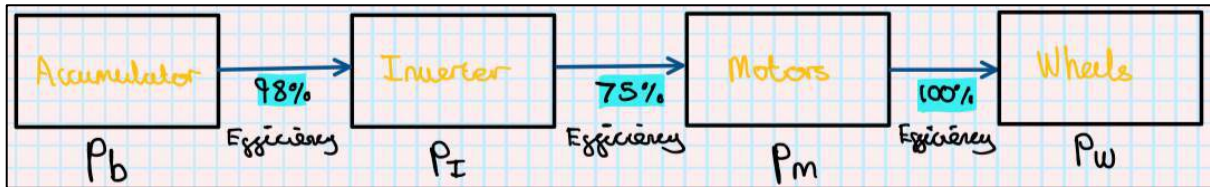


Figure 5 Efficiency values: Accumulator, inverter, motors, wheels.

As the ULM016 incorporates in-hub motors, the efficiency of the wheels to the motors are assumed to be 100%, i.e.  $P_w = P_m$ . The power requirement at the inverter,  $P_I$ , and the power requirement at the battery,  $P_b$ , can be seen in equation 7 and 8 respectively.

$$P_I = \frac{P_m}{0.75} \quad (7)$$

$$P_b = \frac{P_I}{0.98} \quad (8)$$

The power at the battery, is then divided by a 1000 to obtain the power in kW and then a graph is plotted of power(kW) vs time. The integral of this graph (area under graph) is equivalent to the required capacity in kW.s.

$$Cap(kWs) = \int_0^t P_b dt \quad (9)$$

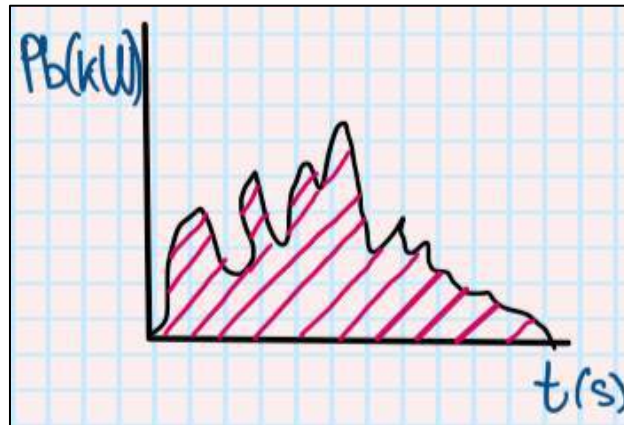


Figure 6 Area under graph of power vs time.

$$Cap(kWh) = \frac{Cap(kWs)}{3600} \tag{10}$$

The output of the code for the required capacity of the battery can be seen in figure 6. Comparing the required capacity with other teams calculations, the range for the endurance event is in the range of 6kWh to 7kWh which demonstrates a level of reliability with the data obtained from this code.

```
Required capacity of the accumulator: 5.51 kWh
Required capacity with FOS of 1.3: 7.17 kWh
```

Figure 7 Required battery capacity to complete endurance event.

### 3.2 Battery cooling requirement calculations

As mentioned previously, the data obtained from the previous calculations are used in the calculations for the simplified thermal model of the battery. Modelling battery temperature without having the experimental temperature data of the cells is very difficult to do because there are many different fluctuating variables based upon changing parameters of the battery; for example, temperature, internal resistance, state of charge(SOC), state of health(SOH), voltage, current and resistance. Many of these parameters are functions of temperature which makes it very difficult to accurately estimate the values. A more accurate method is to model an equivalent circuit of the battery using a Simulink package called Simscape Electrical.

### 3.2.1 PCM (phase change material).

Phase change material is commonly used in batteries as a heat sink material for the cells. It can store large amounts of heat per unit volume, mainly due to the phase change transition stage. There are four main types of PCM material which include paraffin wax, non-paraffin organics, hydrated salts and metallics (4). Paraffin wax is the most common PCM used due to its high latent heat and stability over phase change cycles. A PCM material must be selected based upon cost, latent heat, density, and the temperature range at melting. It is important to determine the maximum temperature of the batteries and select a PCM material that has a melting temperature of several degrees less than this maximum temperature. This prevents the battery from overheating by absorbing energy in the transition stage as demonstrated by figure 8.

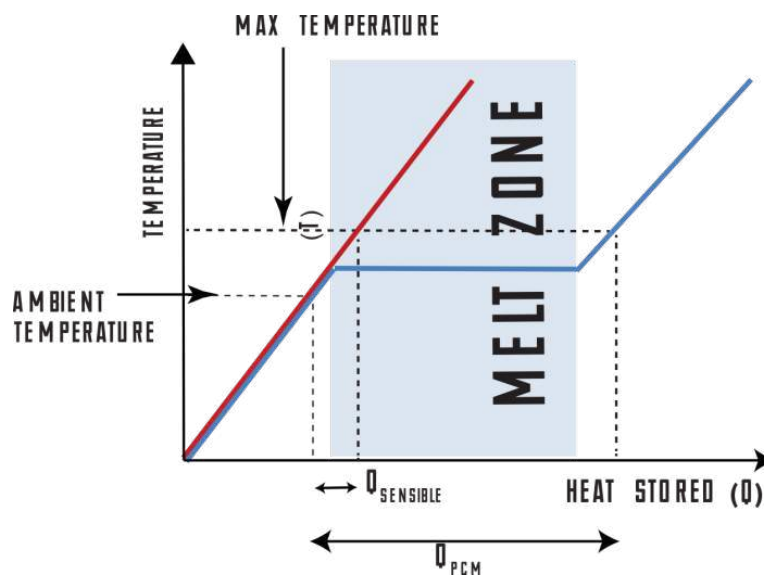


Figure 8 Phase transition stage demonstrating absorption of heat energy (4).

### 3.2.2 Simplified thermal model for lithium ion battery.

This model is based upon the use of a phase change material but it can be simplified further in the event of the use of a simple heat sink material, such as Nomex thermal insulating sheet. Figure 8 demonstrates the thermodynamic heat transfer for the battery. Equation 11 is how to model the temperature change from the battery to the PCM material (5).

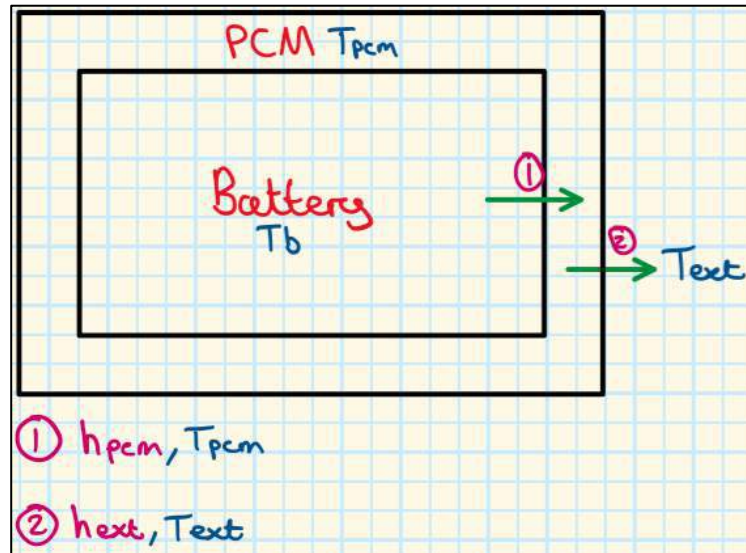


Figure 9 Thermodynamic model of heat transfer in battery.

$$(mc_p)_{pcm} \frac{dT_{pcm}}{dt} = h_{pcm}A_b(T_b - T_{pcm}) + h_{ext}A_{ext}(T_{ext} - T_{pcm}) \quad (11)$$

The change in temperature of the PCM material over time can be determined from equation 11. The PCM material can then be selected based upon the increase in temperature of the PCM. In order to calculate this temperature increase, the temperature of the battery must be determined with respect to time using Simscape electrical.

$$C_{p,pcm}(T) = C_{base}(T) + L_s \frac{\frac{2\gamma}{\Delta T}}{\pi \left[ \left( (T - T_m) \left( \frac{2\gamma}{\Delta T} \right) \right)^2 + 1 \right]} \quad (12)$$

Equation 12 describes how the specific heat capacity of the PCM can be calculated using the ambient temperature of the PCM and the phase change temperature range.

### 3.2.3 Simscape electrical.

As mentioned previously, because of the difficulty of modelling battery temperature due to the numerous parameters of the battery that are functions of temperature using Simscape electrical is the most accurate method to model the varying parameters of the battery.

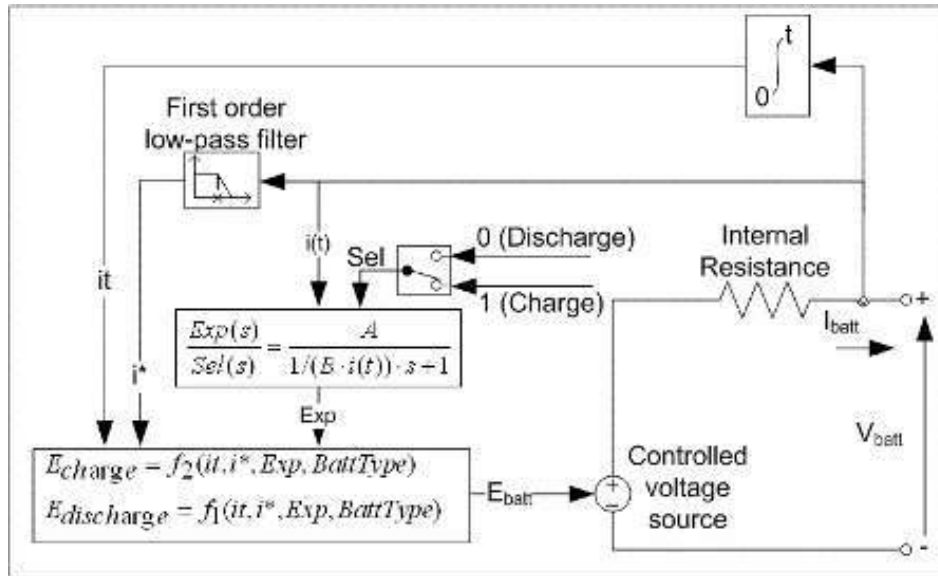


Figure 10 Generic equivalent circuit battery model setup on Simscape Electrical.

Many equations must be used to set up the battery model in figure 10 but the equations below model the battery temperature with respect to time (6). The data obtained from this can then be used in equation 11 to determine the change in temperature of the PCM. The full equations for this model can be seen in appendix B.

$$T_b(t) = L^{-1} \left( \frac{P_{loss} R_{th} + T}{1 + s \cdot t_c} \right) \quad (13)$$

## 6 References

1. **DOBER.** LITHIUM-ION BATTERY PACKS & METHODS OF COOLING THEM. *DOBER*. [Online] 2020. [https://www.dober.com/electric-vehicle-cooling-systems#electric\\_vehicle\\_thermal\\_management\\_system](https://www.dober.com/electric-vehicle-cooling-systems#electric_vehicle_thermal_management_system).
2. **Martellucci, L. and Giannini, M.** *Regenerative Braking Experimental Tests and Results for Formula Student Car*. Italy : Journal of Transportation Technologies, 2021.
3. **Ghabech, C., Yadav, A.K., Khaligh, A., Singhabahu.** *Systematic Modelling and Design of a Battery Pack for Formula Electric Vehicles*. s.l. : SAE Technical Paper, 2021.
4. **ACT.** Phase change material (PCM) selection. *ADVANCED COOLING TECHNOLOGIES*. [Online] March 2021. [Cited: 3rd February 2022.] <https://www.1-act.com/products/pcm-heat-sinks/pcmselection/>.
5. **Bilal Lamrani, Badr Eddine Lebrouhi.** *A simplified thermal model for a lithium-ion battery pack with phase change material thermal management system*. Morocco : ELSEVIER, 2021.
6. **MathWorks.** Battery. *MathWorks*. [Online] 2021. <https://uk.mathworks.com/help/physmod/sps/powersys/ref/battery.html>.
7. **RS .** RS PRO Adhesive, 25ml. *RS*. [Online] 2022. [https://uk.rs-online.com/web/p/adhesives/0850962?cm\\_mmc=UK-PLA-DS3A--google--CSS\\_UK\\_EN\\_Adhesives\\_%26\\_Sealants\\_%26\\_Tapes\\_Whoop--Adhesives\\_Whoop--850962&matchtype=&pla-300138803990&gclid=CjwKCAiAl-6PBhBCEiwAc2GOVDX808085FInMlgl-EtWGNyixL2RI6HvldrnbIV5U0](https://uk.rs-online.com/web/p/adhesives/0850962?cm_mmc=UK-PLA-DS3A--google--CSS_UK_EN_Adhesives_%26_Sealants_%26_Tapes_Whoop--Adhesives_Whoop--850962&matchtype=&pla-300138803990&gclid=CjwKCAiAl-6PBhBCEiwAc2GOVDX808085FInMlgl-EtWGNyixL2RI6HvldrnbIV5U0).
8. **Andor.** PCM Phase Change Cooling Material For Li-Ion Battery Pack Battery. *ANDOR*. [Online] February 2022. <https://www.andores.com/sale-13853703-pcm-phase-change-cooling-material-for-li-ion-battery-pack-battery.html>.
9. **FSUK.** Institution of mechanical engineers. *Formula student UK*. [Online] 2021. <https://www.imeche.org/events/formula-student/team-information/rules>.

## 7 Appendix

### 7.1 Appendix A: Python code for capacity calculation

```
1 # Cell and module selection
2 import numpy as np
3 import pandas as pd
4 import matplotlib.pyplot as plt
5 from scipy.integrate import trapz, cumtrapz
6 import matplotlib as mpl
7 import pathlib
8
9 working_directory = pathlib.Path(__file__).parent
10
11 # Change font size for all figures
12 mpl.rcParams.update({'font.size': 22})
13
14
15 # Instructions:
16 # 1. Add your speed-time data into the drive cycle sheet of the excel spreadhseet. Make sure this is speed (mph) - time (seconds)
17 # 2. Add your car data in the the car data sheet of the excel spreadhseet
18 # 3 Run the script.
19 #####
20 # speed-time data graph
21 speed_data = pd.read_excel(
22     working_directory/'Car data.xlsx', sheet_name='drive cycle')
23
24 time_s = np.array(speed_data.iloc[0:, 1])
25 speed_mph = np.array(speed_data.iloc[0:, 0])
26
27
28 plt.figure(figsize=(10, 10))
29 plt.plot(time_s, speed_mph)
30 plt.xlabel('Time (seconds)')
31 plt.ylabel('Speed (mph)')
32 plt.title('Speed vs Time')
33 plt.show()
34 #####
35 # Model of forces on car
36 car_data = pd.read_excel(
37     working_directory/'Car data.xlsx', sheet_name='car data')
38
39 speed_ms = np.array(speed_data.iloc[0:, 0])/2.237 # speed in m/s
40
41 # Car parameters
42 air_den = car_data.iloc[0, 1] # air density (kg/m3)
43 fro_area = car_data.iloc[1, 1] # frontal area (m^2)
44 roll_res_co = car_data.iloc[2, 1] # Rolling resistance coefficient
45 car_mass = car_data.iloc[3, 1] # Total mass of car with driver (kg)
46 air_speed = car_data.iloc[4, 1] # assumed 0 for now
47 track_fric = car_data.iloc[5, 1] # coefficient of friction of track
48 motor_eff = car_data.iloc[6, 1] # Motor efficiency #need to workout
49 drag_coe = car_data.iloc[7, 1] # Drag coefficient #need to check
50 inv_eff = car_data.iloc[8, 1] # inverter/motor controlled efficiency
```

```

52 # Calculation of aerodynamic drag
53 # Aerodynamic drag(N)
54 drag_resis = np.array((air_den*fro_area*drag_coe*(speed_ms)**2)/2)
55
56 # Speed (m/s) vs Time (s) graoh
57
58 #plt.figure(figsize=(100, 4))
59 #plt.xticks(np.arange(min(time_s), max(time_s)+1, 5))
60 plt.figure(figsize=(10, 10))
61 plt.plot(time_s, speed_ms)
62 #plt.figure(figsize=(6, 4))
63 #plt.xticks(np.arange(min(time_s), max(time_s)+1, 5))
64 plt.xlabel('Time (seonds)')
65 plt.ylabel('Speed (m/s)')
66 plt.title('Speed vs Time')
67 plt.show()
68
69
70 # Aerodynamic drag resistance graph
71 plt.figure(figsize=(10, 10))
72 plt.plot(time_s, drag_resis)
73 plt.xlabel('Time (seonds)')
74 plt.ylabel('Drag resistance (N)')
75 plt.title('Drag resistance vs Time')
76 plt.show()
77
78 # Rolling resintance force
79 # instead of 0 for angle, need (gradient of track) at different points.
80 roll_res = roll_res_co*car_mass*9.81*np.cos(0)
81
82 # Gradient resistance force
83 grad_res = car_mass*9.81*np.sin(0) # need gradient (angle) again
84
85 # Required tractive force to achieve certain acceleration
86 # Not sure if this is correct.
87 acceleration = np.nan_to_num(np.gradient(speed_ms, time_s))
88 acc_force = car_mass*acceleration # Force due to acceleration
89 trac_force = np.array(drag_resis + roll_res + grad_res +
90                       acc_force) # tractive force
91 # remove negatives from trac_force as no power required from accum to decelerate.
92 trac_force[trac_force < 0] = 0
93 #####
94 # Power requirement calculations
95
96 # Power demand at wheels
97 power_whe = trac_force*speed_ms # power requirement at wheels
98 power_inv = power_whe/motor_eff # power requirement at inverter
99 power_acc = (power_inv/inv_eff)/1000 # power requirement at accumulator
100

```

```
101 #plt.figure(figsize=(120, 4))
102 #plt.xticks(np.arange(min(time_s), max(time_s)+1, 5))
103 plt.figure(figsize=(10, 10))
104 plt.plot(time_s, power_acc)
105 plt.xlabel('Time (seonds)')
106 plt.ylabel('Power requirement of accumulator (kW)')
107 plt.title('Power vs Time')
108 plt.show()
109
110 #####
111 # Capacity requirement of accumulator calculation
112 energy = "{:.2f}".format(trapz(power_acc, time_s)/3600)
113 energy2 = np.ceil(energy*1.3)
114 print('Required capacity of the accumalator: '+str(energy) + ' kWh')
115 print('Required capacity with FOS of 1.3: ' + str(energy2) + ' kWh')
116 #####
```

### 7.1.1 Simplified code explanation

Accumulator simulation capacity explanation

Simple needed eqs

- $F_{air}$  and  $F_{air}$  both changing with different velocities/acc

$F_{air} = \frac{\rho_{air} A_f C_d (V + V_{air})^2}{2}$  → Drag resistance =  $\frac{\text{density of air} \times \text{frontal area} \times \text{drag coefficient} \times \text{speed}^2}{2}$

$F_r = \mu_r M g \cos(\alpha)$  → Rolling resistance =  $\text{friction coefficient} \times \text{car mass} \times g \times \cos(\alpha)$

$F_g = M g \sin(\alpha)$  → Gravity resistance =  $\text{Car mass} \times g \times \sin(\alpha)$

$F_a = M \frac{dv}{dt}$  → Acceleration force =  $\text{Car mass} \times \text{acceleration}$

Assumptions for now:

- Velocity of air ( $V_{air}$ ) = 0
- Gradient of track = 0

Total force acting on car

$$M \frac{dv}{dt} = F_t - (F_g + F_r + F_{air})$$

$$F_t = M \frac{dv}{dt} + (F_g + F_r + F_{air})$$

- $F_t$  = **Traction force** required to meet desired acceleration.
- If  $F_t < 0$  → Car braking → not using power from battery
- For values of  $F_t < 0 \rightarrow 0$  (change all negative values to zero)

Power calculations

- $P_m = P_w$  → In hub design
- $P_m = F_t \times V$
- $P_e = \frac{P_m}{0.75}$
- $P_b = \frac{P_e}{0.98}$
- $P_b \rightarrow W \rightarrow kW$
- $\text{Cap}(kWh) = \int_0^t P_b dt$
- $\text{Cap}(kWh) = \frac{\text{Cap}(kWh)}{60 \times 60}$



SCHOOL OF ENGINEERING

YEAR 3 INDIVIDUAL PROJECT

**FINAL REPORT**

***Novel ultrafilter water purification  
system for Luanda, Angola.***

133/6

Christopher Cooper

MEng

29/03/2021

Supervisor: DSA Raechelle

## **Summary**

The aim of this project is to develop the design of a pump based filtration system that will be suitable for transportation, filtration and storage of water from the Kwanza, Bengo and Dande rivers in the rural Luanda regions of Angola. The actual filtration process is based upon the report '**Quality assessment of water intended for human consumption from Kwanza, Dande and Bengo rivers (Angola)**'. In this quality assessment report, it outlines the spatial and temporal distribution of the contaminant's in this region along with recommend treatment processes based upon the WHO guidelines. The design of the novel purification system is driven by engineering science, the contaminant data and the WHO guidelines for household water treatment. The idea was to produce a design that would be competitive with the LifeStraw community product. The main findings were that in the Luanda region, during the rainy season the biggest issue in terms of water treatment was faecal matter. With this issue, one of the main difficulties with design process was finding a balance between effectiveness of the filtration and the cost and ease of use/maintenance of the treatment process for the design context. A polyester pre-filter was selected a long with a hollow fibre ultrafilter for the best balance between the parameters mentioned above. Further testing would need to done on the specific ultrafilter to determine the effectiveness of reducing the abundance of faecal matter. If ineffective based upon the WHO guidelines, then chemical treatment with sodium hypochlorite would be required.

### *Table of notation*

<b>Symbol</b>	<b>Represents</b>	<b>[Units]</b>
$A_{cyl}$	Area of the cylinder	[m <sup>2</sup> ]
$D_{hose}$	Diameter of hose	[m]
$F_c$	Suction force of vacuum	[N]
$F$	Force from spring on piston	[N]
$h_{cyl}$	Height of cylinder	[m]
$k$	Spring stiffness	[N/m]
$L_{hose}$	Hose pipe length	[m]
$m$	Mass of displaced water.	[kg]
$\dot{m}$	Mass flow rate	[kg/s]
$n$	Efficiency of pump.	[No units]
$P$	Power of the pump	[W]
$\Delta p$	Pressure to pump fluid	[Pa]
$Q$	Volumetric flow rate	[litres/min]
$R_{cyl}$	Radius of cylinder	[m]
$t$	time	[s]

$V_{\text{cyl}}$	Volume of pump cylinder	$[\text{m}^3]$
$W_s$	Factor of safety	[No units]
$x$	Displacement of spring	[m]

### 2.3 Data and discussion

The data collected for these parameters in the 'Quality assessment of water' report determined that during the dry season, A2 class treatment is suitable for producing good quality drinking water. However, during the rainy season, the rainfall-runoff moves lots of organic pollutants into the rivers and faecal matter. If low enough, the BOD (biological oxygen demand) usually infers that there is a sufficient amount of oxygen for bacteria to degrade the organic pollutant. However, this parameter was recorded much higher during the rainy season and the concentrations of the other ions and especially faecal coliforms. An A3 class treatment would be required to remove dissolved organic and nutrient compounds. The data collected from this report can be seen in appendix B.

## 3 Concept development

### 3.1 Concept 1

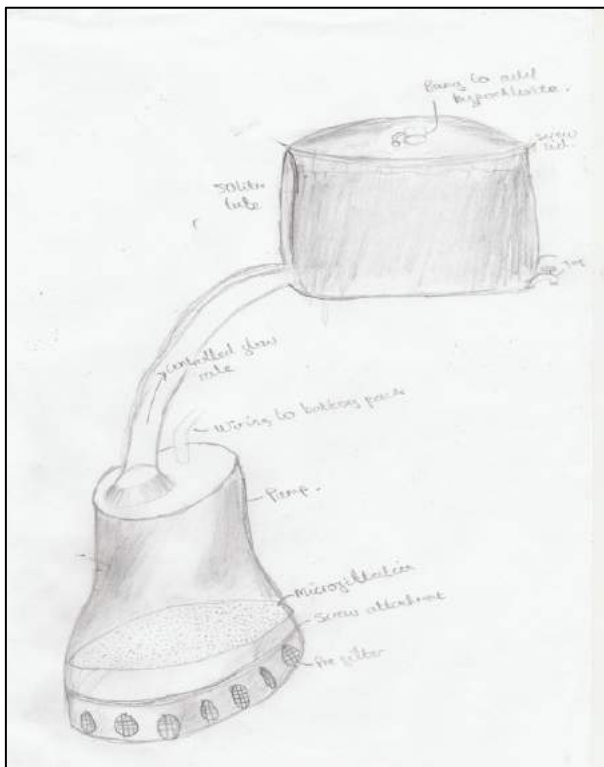


Figure 2 Water turbine pump filtration unit to tank.

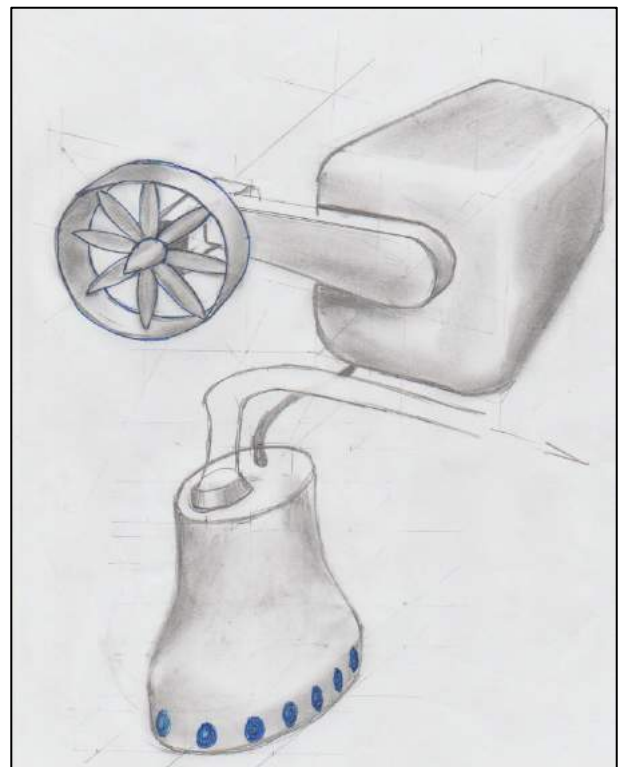


Figure 3 Water turbine pump filtration unit.

The design is a water turbine that generates electricity to power a pump filtration unit that contains a hollow fibre microfilter membrane. As microfilters can not remove viruses, further chemical disinfection (sodium hypochlorite) would be required to remove any further pollutants that fail to be removed from the microfilter. This would have to be done in a measured 50 litre tank that the connecting pipe leads to. This concept could act as a

temporary replacement to the unreliable taps in the Luanda region.

However, some of the issues with this design in order for it to be practical, the piping would have to travel over very large distances of 5km and therefore it would be very hard to design a pump that will be able to maintain a high enough pressure to move the water over these distances. A shorter distance could be used but this would be impractical as it doesn't suit the context of the region of Luanda. Maintenance would also be very difficult as the design will be very complex due to all of the electronics involved with a water turbine.

Manufacturing to have a water tight container for the electronic components would be very difficult and would require lots of testing and a large budget.

### 3.2 Concept 2

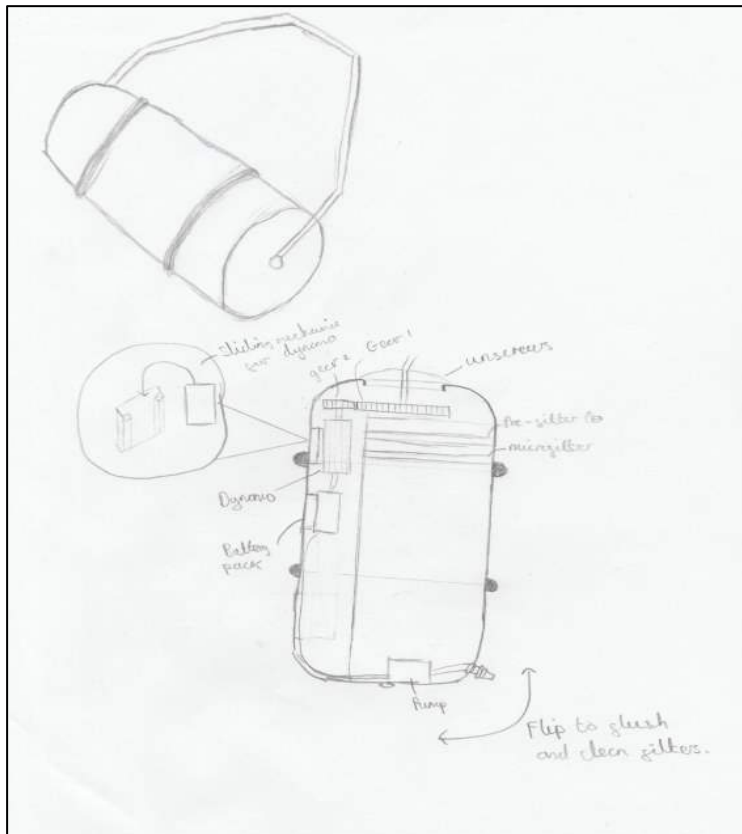


Figure 4 Initial rollable water purification system design idea.

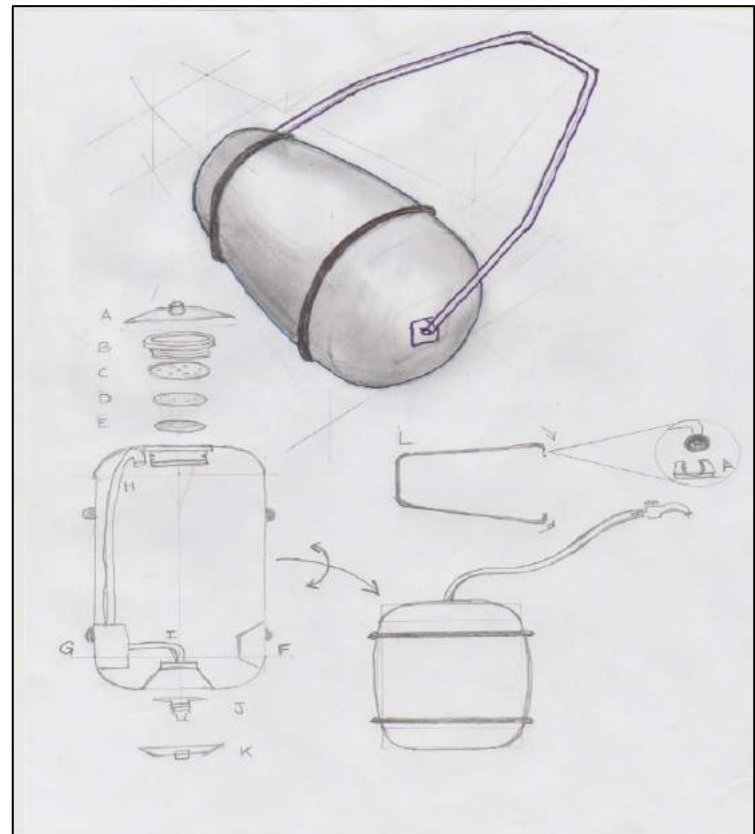


Figure 5 Rollable water purification design iteration.

In the first sketch, the design is a 50-litre rollable water tank. Gear 1 is static and attached to a dynamo that generates electricity, when rolling, stored in a battery. The battery can then power a pump after the water is filtered through a two-stage filtration unit. The lid is unscrewed at the top and water is poured down a removable funnel onto a pre-filter that removes any of the larger particles. The water then travels through a microfilter where the

water can be pumped out. There are many issues with this design. The DFMA (design for manufacture) is very bad as there are many loose parts and easily breakable parts. The filtration process would also not be efficient in removing the contaminants mentioned previously in the reports. The design would also make it very difficult to replace the filters or remove particulate matter from the filters.

In the second sketch, the design is much more simplified with the lid A, B, C, D and E being the filtration unit. This uses an ultrafilter and chlorination to produce safe drinking water. Once the water is passed through the filter, hydro chlorite can be added in a measured amount and then the tank can be flipped over. A hosepipe attachment is then exposed under the lid at the top (J, K) to use the water. A pump is used to move the water through the pipes. The filters can be easily flushed or replaced with them being integrated with the lid of the tank.

## 4 Detailed design

### 4.1 Final design

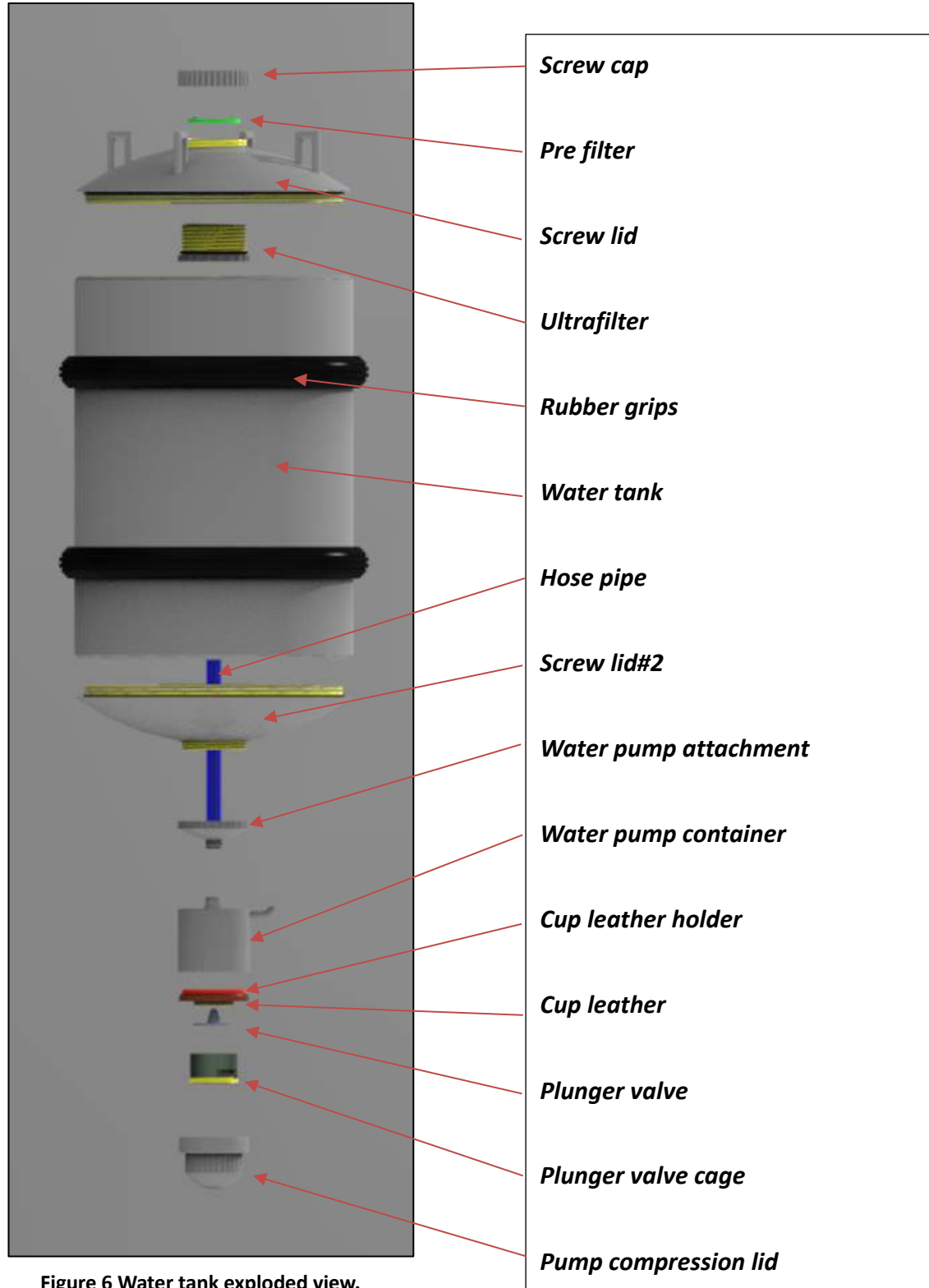
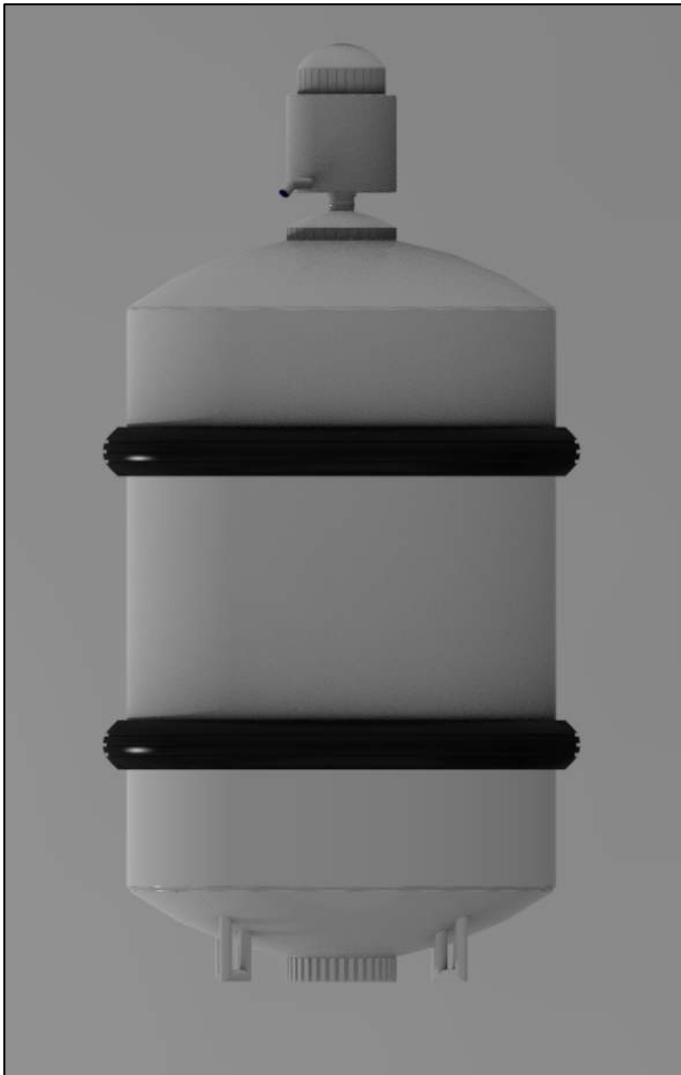
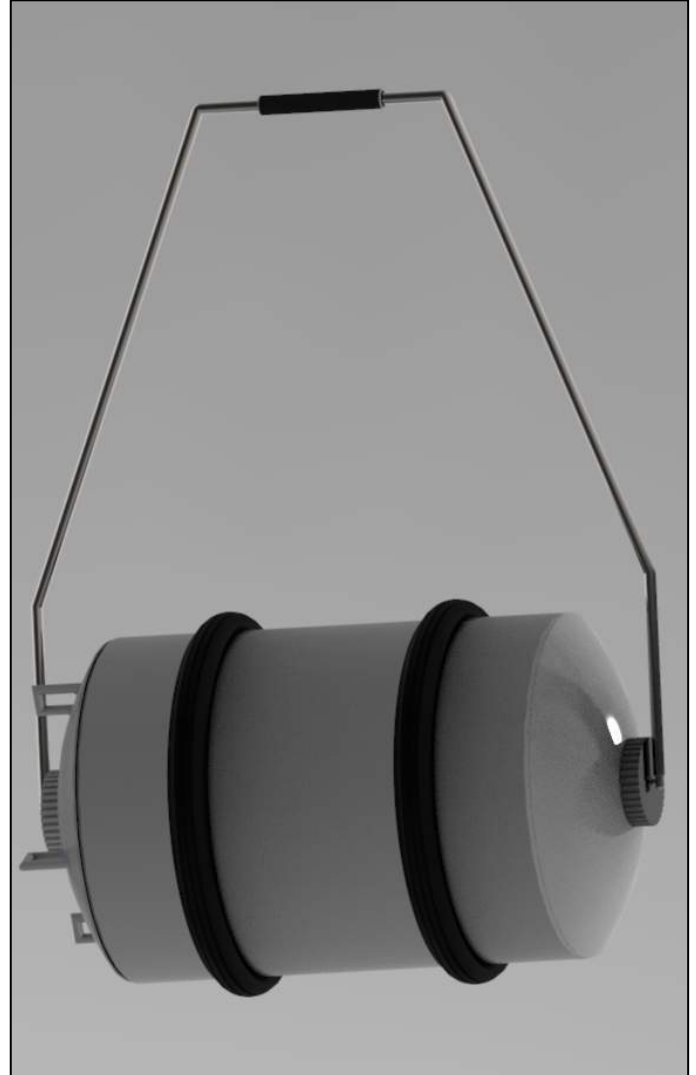


Figure 6 Water tank exploded view.



**Figure 7 Water tank with pump.**



**Figure 8 Water tank in portable mode.**

At the river bank, water would be poured onto the pre-filter where the water will then slowly filter through the ultrafilter into the sealed water tank. Once full, the screw cap would be screwed onto the water tank and then the handle for the tank would be assembled as shown in figure 7. The tank can then be rolled back to the persons household and the hand pump can be attached as shown in figure 7 to use the clean water in the tank. Care should be taken to remove and rinse the pre-filter and ultrafilter with clean water after each use to prevent build ups of contaminants. For the design context, this device would be very useful to local communities in the Luanda region. It produces safe and clean water while making it very convenient and cost affective to attain clean drinking water. The design is very easy to assemble with colour co-ordinated components and it has very simple maintenance.

## 4.2 Pre-filter and Ultrafilter

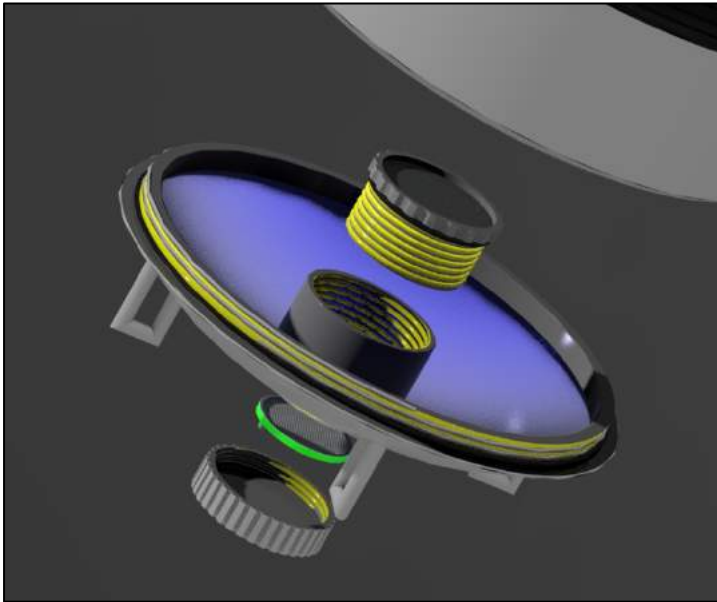


Figure 9 Filter assembly (angle 1).

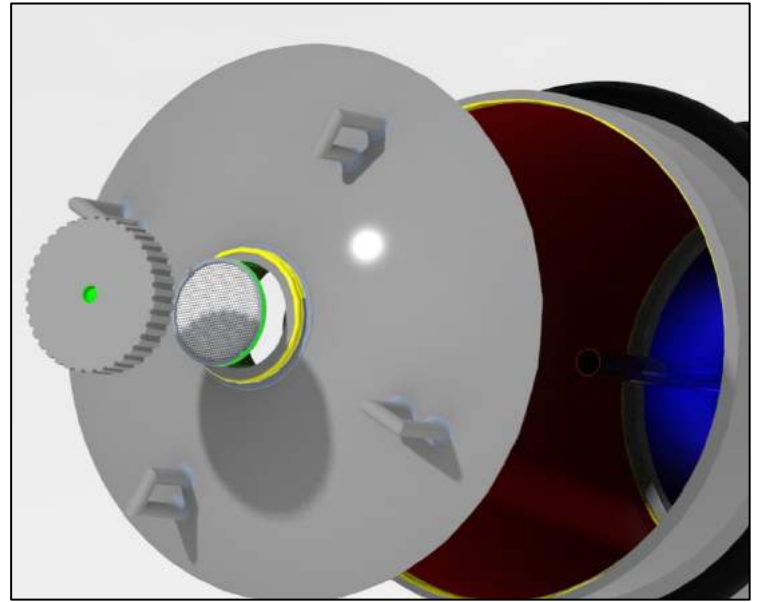


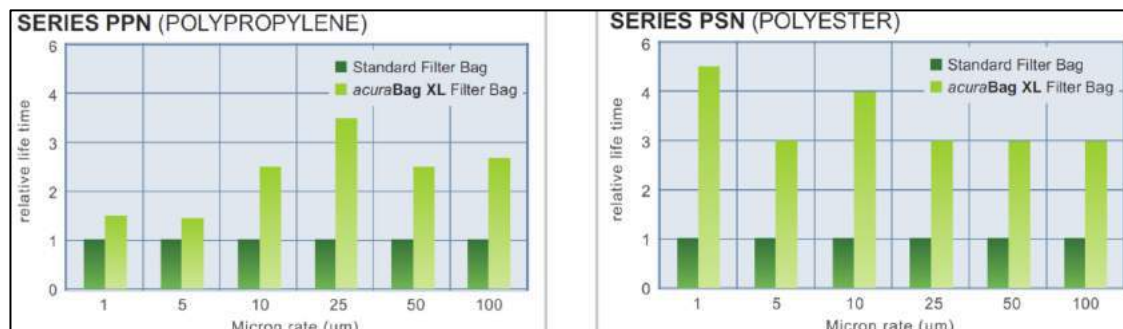
Figure 10 Filter assembly (angle 2).

### 4.2.1 Pre-filter

As seen in figure 9 and 10 the pre filter sits within the top of the screw lid and is encapsulated by the screw cap. The pre filter is made out of a very thin mesh membrane that removes any particles larger than 80 microns. The actual mesh filter material can be outsourced and it is made of polyester felt. This material allows for a high flow rate of  $45\text{m}^3/\text{h}$  through the mesh while being a long lasting durable material for filtration (sigafiltration, 2019). The polyester also has a high operating temperature (120 degrees Celsius) in the event that further processing of water would be needed such as boiling the water and then passing it through the filter. This further processing maybe needed during the rainy season to lower the abundance of faecal coliform in the water but more testing would be needed to confirm this.

Alternatives to the polyester material is polypropylene however the operating temperature of this material is only 90 degrees Celsius. If users boiled the water before passing it through the filter, the material would get damaged. Polyester filters also have a longer life time compared to polypropylene as shown by the graphs below.

This pre-filter would need to be rinsed after use to remove any particulate matter and once clogged the pre-filter would need to be replaced. This lifetime could range from 8000 to 9000 gallons replacement or replace every twelve months (APEC, 2012)



Graph 2 Pre-filter material life time comparison.

#### 4.2.2 Ultrafilter

An ultrafilter was selected due to contaminants discussed in the contaminant review. Ultrafilters are very effective in removing bacteria, parasites viruses and microplastics. With the recommend processes in the contaminant review, coagulation, flocculation, sedimentation and chlorination, ultrafiltration can completely replace these processes (Wikipedia, 2019). This greatly reduces the time of the treatment process and the cost. As the rivers during the rainy season contain a significant amount of dissolved organic pollutants and faecal matter, ultrafiltration was chose over microfiltration due to its ability in removing these pollutants (Jr., 2012). However, depending on the concentration of faecal matter, the ultrafilter may not be fully effective in removing this pollutant to the guidance values in the WHO guidelines. This is especially apparent in gravity filtration ultrafilters (Chaidez, 2016). Further testing would be required specific to the designed ultrafilter to determine the abundance of faecal matter after the filtration. If insufficient, sodium hypochlorite would be needed to reduce the abundance of faecal matter.

There are different types of ultrafiltration membrane arrangements that filter different levels of parameters and that require different temperatures and pressures to complete the filtration. This is summarised in the table below.

Table 5 Parameters for different membrane arrangements.

	Hollow Fibre	Spiral-wound	Ceramic Tubular
pH	2–13	2–11	3–7
Feed Pressure (psi)	9–15	<30–120	60–100
Backwash Pressure (psi)	9–15	20–40	10–30
Temperature (°C)	5–30	5–45	5–400
Total Dissolved Solids (mg/L)	<1000	<600	<500
Total Suspended Solids (mg/L)	<500	<450	<300
Turbidity (NTU)	<15	<1	<10
Iron (mg/L)	<5	<5	<5
Oils and Greases (mg/L)	<0.1	<0.1	<0.1
Solvents, phenols (mg/L)	<0.1	<0.1	<0.1

A hollow fibre membrane was selected mainly because of the feed pressure. As shown in table 5, the hollow fibre membrane can be used at ambient air pressure (14.7psi). The membrane consists of thousands of hollow fibres that are cleaned by back flushing water through the filter. The material selected for this membrane arrangement was polypropylene due to its very low density ( $0.92\text{g/cm}^3$ ) and its ability to be integrated to other plastic parts, for example the casing on of the ultrafilter (wikipedia, 2018).

**Amount of chlorine required:**

Chlorination of water is a well-established and reliable method to purify drinking water. This method of purification has proved effective against a wide variety of pathogens commonly found in drinking water. Chlorine is able to damage cell membranes and subsequently enter the cells and disrupt respiration and DNA activity. It can effectively be used to remove faecal matter.

It should be noted that high levels of chlorine in drinking water can be harmful. As such, the World Health Organisation has set a limit of 5mg of chlorine residual per litre of water as maximum safe concentration for human consumption (DWI, 2010). In the interest of safety, 2mg/L has been deemed an appropriate concentration to disinfect water and avoid over-chlorination.

Sodium hypochlorite can be used to purify drinking water according to the following procedure.

1. Add 200mg of sodium hypochlorite (NaOCl) to 1 litre of water. Stir this solution until the sodium hypochlorite is completely dissolved. The resulting concentrated solution can be used to disinfect multiple tanks of water.

$$c_{concentrated} = \frac{200\text{mg}}{1\text{L}} = 200\text{mg/L} \quad (1)$$

2. Mix 1 part concentrated solution with 100 parts water. For a 50L tank, 0.5L (500ml) of concentrated solution should be added. The water should be stirred thoroughly to allow the concentrated solution to mix with the water.

$$c_{dilute} = \frac{200\text{mg}}{1} \times \frac{0.5\text{L}}{50\text{L}} = 2\text{mg/L} \quad (2)$$



Out of the materials displayed on the graph, polyethylene can be seen to have the lowest density and price and therefore this material was selected for the casing. It is very easy to mould and it can come in a wide range of colours. The material properties can be seen in appendix A.

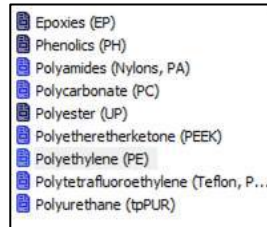


Figure 11 Materials from selection (Granta,2021).

### 4.3 Water tank with screw lids.

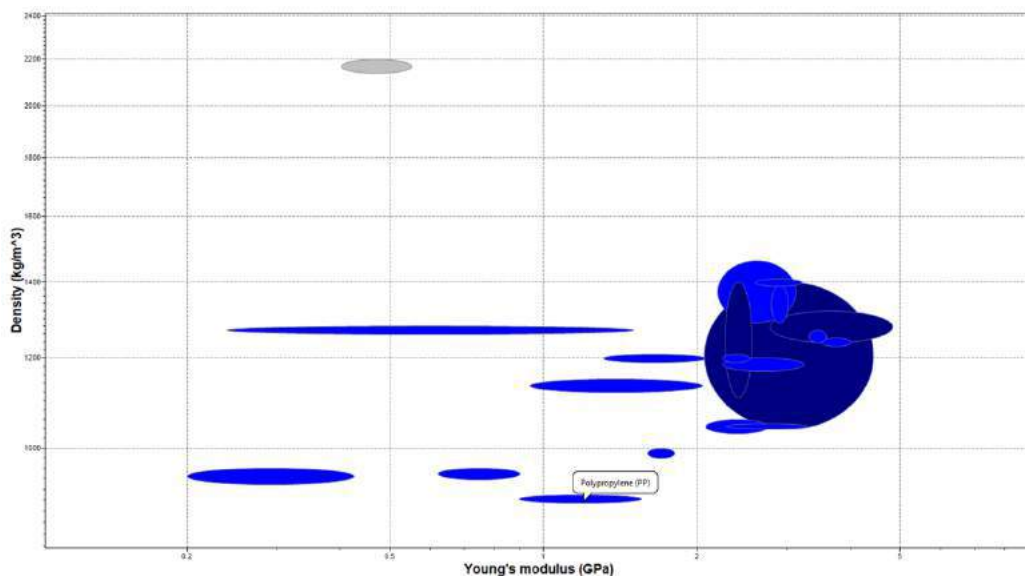
The water tank has a 50 litre capacity. The most important design parameters for the tank and the screw lids is the material. It has to be a material that has ideal mechanical properties; lightweight, high young's modulus, high compressive strength, high impact strength and easily moulded. It also has to be as cheap as possible. Most of these water tanks are made of polymers due to durability and cost. Other 50 litre water tanks available on the market have the properties listed below.

- Compressive strength – 20Mpa – 90MPa.
- Impact strength –  $1.5 \times 10^5$  J/m<sup>2</sup>–  $2.2 \times 10^5$  J/m<sup>2</sup>.
- Youngs modulus –  $1.05 \times 10^9$ - $1.10 \times 10^9$  Pa (Choe, 2004).
- Cost - £0 - £3 per kilogram

The most important parameters for my design is the young's modulus and the density. The graph below displays the balance between these parameters for all the polymers with the mechanical properties above. All of the materials determined from the selection process can be seen in figure 12.

- Acrylonitrile butadiene styrene (A...
- Cellulose polymers (CA)
- Epoxies (EP)
- Ionomer (I)
- Phenolics (PH)
- Polyamides (Nylons, PA)
- Polycarbonate (PC)
- Polyester (UP)
- Polyethylene (PE)
- Polyethylene terephthalate (PET)
- Polyhydroxyalkanoates (PHA, PHB)
- Polylactide (PLA)
- Polymethyl methacrylate (Acrylic, ...)
- Polyoxymethylene (Acetal, POM)
- Polypropylene (PP)
- Polystyrene (PS)
- Polyurethane (tpPUR)
- Polyvinylchloride (tpPVC)
- Starch-based thermoplastics (TPS)

Figure 12 Polymer materials from selection.



Graph 4 Polymers - Density VS Young's modulus.

As shown on graph 5, polyethylene (PE) was selected due to its low density and high Young's modulus. This is the same material for the casing of the filters. The material properties can be seen in appendix A. As mentioned before, polyethylene is non-toxic and it can be moulded very easily. There are three different types of PE which include low density polyethylene (LDPE), medium density (MDPE) polyethylene and high density polyethylene (HDPE). Successively, the chains of the different types of PE become longer and less branched making them much stiffer and stronger. HDPE is usually used for containers and pipes, so this was selected for the material of the water tank and the screw lids (Kamal

B.Adhikarya, 2016).

#### 4.4 Water pump

The assembly of the hand pump can be seen in figure 12 and 13. Most of the components shown in figure 12 are screwed onto each other except for the plunger valve cup leather holder and the cup leather. Essentially, the compression lid is pressed down and the cup leather holder presses on the spring.

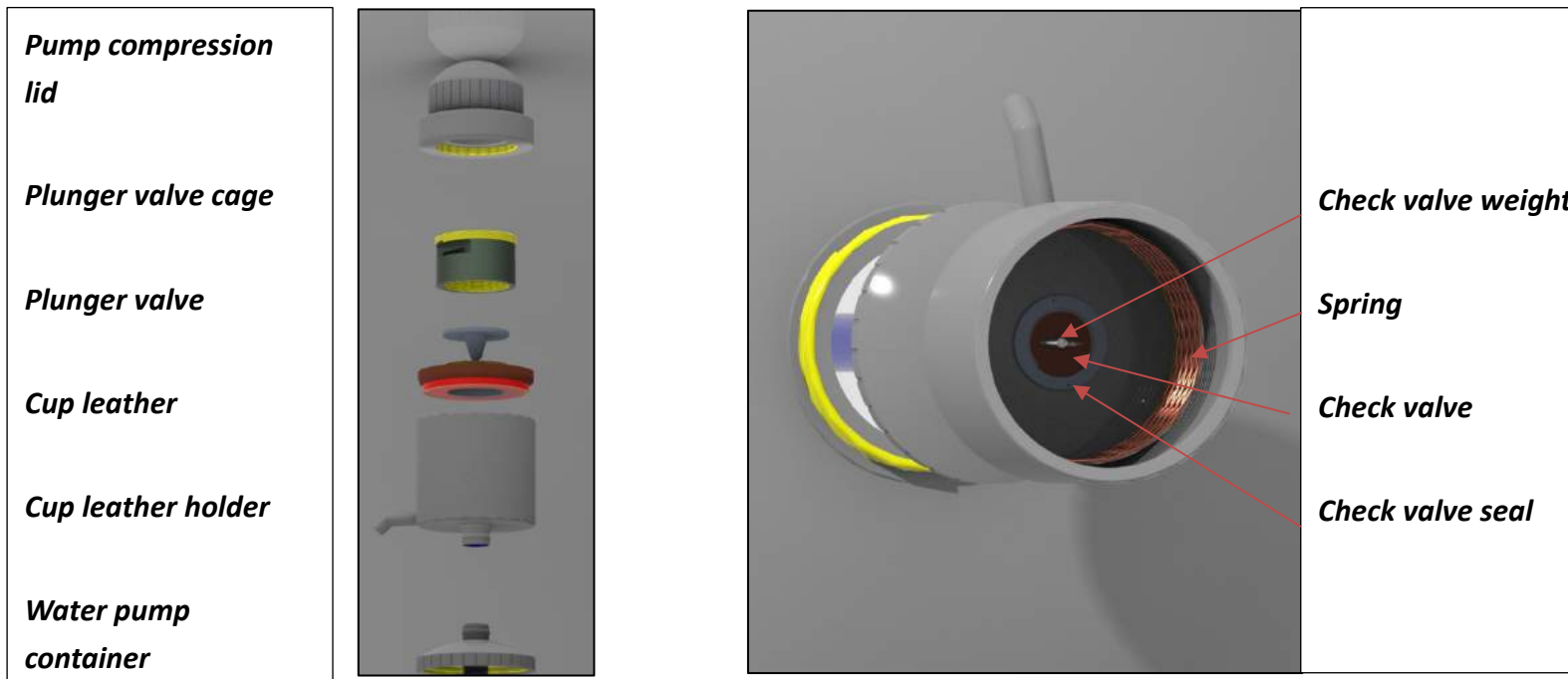


Figure 13 Pump components.

Figure 14 Inside pump.

The cup leather is the same diameter as the water pump container and on the rebound of the lid, a vacuum is created inside the pump that creates a change in pressure which creates a force that pulls up the water. Water gets pulled up through the hose pipe and once at the top it lifts the check valve and the weight to allow water to pass through. The water pump container can then fill with water and allow water to be collected. The plunger valve is encased by the plunger valve cage and can move vertically, up and down, to allow water to pass through to collect more water.

##### 4.4.1 Engineering science calculations

The design decision made when creating this was based upon the engineering science behind reciprocal hand pump and the forces involved with vacuums and springs.

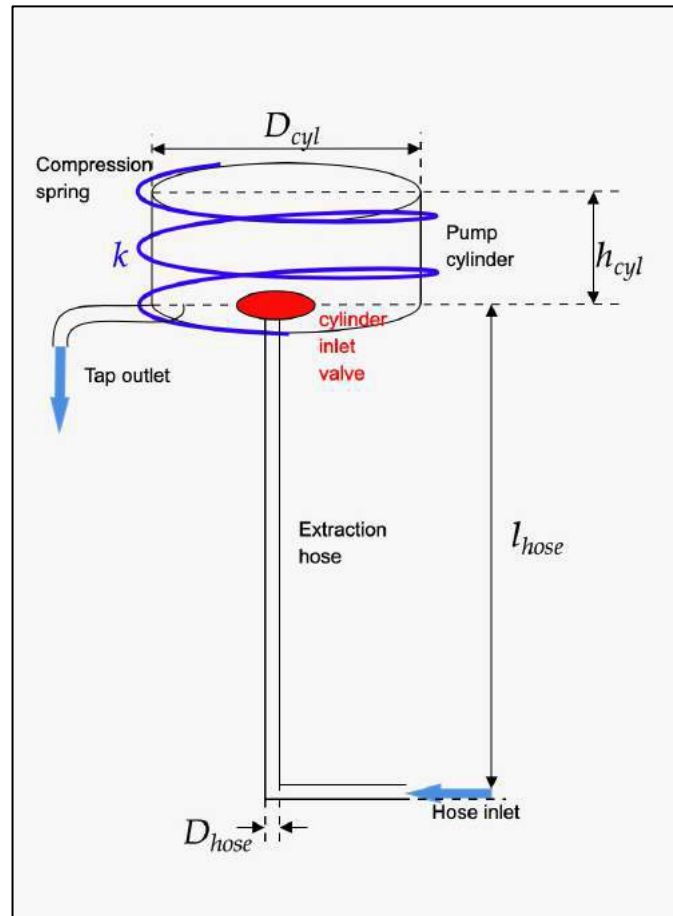


Figure 15 FBD of pump and piping.

**Power requirement of pump:**

The capacity of the drum is 50l. A pump is used to efficiently and reliably dispense water from the vessel via a tap. The decision was to utilise a tap that is situated on the top of the vessel when it is in an upright position is because it avoids the possible contamination that might occur if the tap were near the base of the vessel. This decision however does necessitate the use of a pumping system that can draw the water from the bottom of the container when it is in the upright position. Whilst this does add additional complexity to the design, which increases the cost of the unit and possibly adds new mechanisms of failure, the pump has been designed to be as simple with as few constituent parts as possible. The use of a tap reduces waste compared to pouring from a container, and by situating this tap at the top of the vessel it avoids any need for users to have to lift the drum in order to dispense water. When full the drum and its contents will weigh more than 50kg.

To design the pumping system, a design criterion was assigned that the pump should be able to entirely empty the vessel in no more that 100 articulations of the pump mechanism. The summary of the engineering calculations undertaken to design the pump system can be

seen below.. The code I developed to compute these parameters is given in the appendix C. The code prints the inferred values given the geometric design criterion I selected. In addition to those I have already described I also have a hose length  $l_{hose} = 550mm$ , a pump cylinder height  $h_{cyl} = 70mm$ , this is also the length of required articulation to achieve one compression of the cylinder. There is also the hose diameter  $D_{hose} = 15mm$ , a pump efficiency  $\eta_{pump} = 90\%$ , and a design safety factor  $\omega_s = 1.2$ . This design factor is applied to the maximum expected required force of the pump to account for any other losses such as the additional friction induced through flow passing through the one-way valve at the cylinder inlet, the calculations have been conducted assuming the hydrostatic pressure is zero, equivalent to the drum being empty. When the drum has a height of fluid in it this contributes to the force of the fluid in the direction of flow through the hose so helps the pump to deliver work.

Specifying the 100 pump empty design criterions means the necessary volume of the pump cylinder is,

$$V_{cyl} = \frac{V_{cyl}}{100} \quad (3)$$

$$V_{cyl} = \frac{50L}{100} = 0.5L = 0.0005(m^3) \quad (4)$$

Another design constraint is assigned that the pump is required to articulate  $h_{cyl}$ , which is 7cm from the maximum to minimum position, so the radius of the cylinder of the pump is,

$$V_{cyl} = R_{cyl}^2 \pi h_{cyl} \quad (5)$$

$$R_{cyl} = \sqrt{V_{cyl} \pi h_{cyl}} = \sqrt{(5E^{-4}m^3) * \pi * .7m} = 0.048(m) \quad (6)$$

Then, assuming an average pump rate of around 20 pumps per minute, the volumetric flow rate is,

$$\dot{Q} = V_{cyl} 20 \quad (7)$$

And the average flow rate is,

$$\dot{m} = \dot{Q}\rho \quad (8)$$

This equates to a flow rate similar to that of a slow tap. This is important because the water may be used for hand hygiene, an issue that has received new prescience as a result of the COVID-19 pandemic. This system is therefore sufficient to be used for that purpose according to WHO guidelines.

$$\begin{aligned} \dot{Q} &= .5 * 20 = 10 \text{ (l/min)} \\ \dot{m} &= 10 * 1E^{-3} * \frac{997}{60} = 0.166 \text{ (kg/sec)} \end{aligned} \quad (9)$$

Then as has been alluded to previously, assuming the drum is empty, so there is no hydrostatic pressure helping the pump dispense the fluid inside the drum. So the required pressure to pump the fluid of  $\Delta P$ , is,

$$\Delta P = \rho g l_{hose} + l_{hose} P_{loss} \quad (10)$$

Where,

$$P_{loss} = \lambda_{pvc} \frac{l_{hose}}{D_{hose}} \frac{\rho}{2} v \quad (11)$$

And the fluid velocity,  $v$ , is calculated from  $\dot{m}$ , by,

$$v = \frac{\dot{m}}{\rho \pi (D_{hose}/2)^2} \quad (12)$$

$$\begin{aligned} v &= 0.166 / (997 \pi (1.5E^{-3}/2)^2) = 0.943 \text{ (m/sec)} \\ \Delta P &= 997 * 9.81 * .55 + .55 * 3251 = 7167 \text{ (Pa)} \end{aligned} \quad (13)$$

Then, the power of the pumping action is on the outward movement of the cylinder, not on the user compression. So, the user applies a force on the downward pressure of the cylinder which loads a spring, and that spring then applies the force to the piston of the cylinder which draws liquid into the chamber. So if the force required is,

$$F = \Delta P A_{cyl} \quad (14)$$

then, the spring constant required is,

$$k = \frac{F}{h_{cyl}} \quad (15)$$

$$k = 7167 * \pi(1.5E^{-3}/2)^2 / 0.7 = 731(N/m)$$

With the safety factor  $\omega$  applied, (16)

$$k = 878(N/m)$$

The full verbose output of the code to compute these parameters is:

```

Cylinder volume: 0.500(l)
Average volumetric flow rate: 10.000(l/min)
                               : 0.167(l/sec)
                               : 1.667E-04(m^3/sec)
pump cylinder radius: 0.048(m)
Avg mass flow rate: 0.166(kg/sec)
Avg flow velocity: 0.943(m/sec)
Pressure of pump : 7167.785(Pa)
Pump Avg power requirement: 7167.785(Pa)
Pump force requirement: 51.198(N)

Spring constant: 731.407(N/m)
With a safety factor: 1.200000
this applied to account for losses and friction!
spring const : 877.688(N/m)
    
```

**Figure 16** Verbose output from code.

## 5 Manufacturing

### 5.1 Bill of materials and costing

Table 6 BOM of water treatment design.

Description	QTY	Material	Weight(Kg)	Manufacturer	Material cost (£)
Screw cap	1	HDPE	0.07144584	Workshop	0.09
Pre-filter	1	polyester +MDPE	0.00215413	Workshop	0.00
Screw lid	2	HDPE	1.92688366	Workshop	2.39
Ultrafilter	1	ppolypropylene +MDPE	0.01925663	Workshop	0.02
Rubber grip	2	Natural rubber	1.52200638	Workshop	1.87
Water tank	1	MDPE	3.71240631	Workshop	4.60
Hose pipe	1	PVC	0.02207614	RS components	0.03
Water pump attachment	1	MDPE	0.04842316	Workshop	0.06
Water pump container	1	HDPE	0.03460281	Workshop	0.04
Cup leather holder	1	MDPE	0.02462791	Workshop	0.03
Cup leather	1	Cow leather	0.00635886	Workshop	0.08
Plunger valve	1	LDPE	0.00799282	Workshop	0.01
Plunger valve cage	1	MDPE	0.04765057	Workshop	0.06
Pump compression lid	1	HDPE	0.18003103	Workshop	0.22
o-ring (326mm)	2	Nitrile rubber	0.0144565	RS components	0.12
o-ring (82mm)	1	Nitrile rubber	0.003237	RS components	0.08
Check-valve seal	1	LDPE	0.00029986		0.10
Check-valve weight	1	Aluminium alloy (Al-Mg)	0.0001539		0.20
Check-valve	1	Cow leather	0.00038701	Workshop	0.10
Spring	1	Stainless steel	0.0339227		0.50
10mm bearing	2	Steel	0.00201451	RS components	4.00
Water roller handle	1	Stainless steel	1.5852704		3.74

Table 7 Mass of the water purification system.

Total mass when portable (without pump)	8.88kg
Total mass when static (with pump)	7.68kg

Table 8 Costing based upon batch size.

	Prototype	5000 batch	30,00 batch
Fixed costs (machinery) (£)	0	10,000	30000
Labour and manufacturing per unit cost (£)	567	113.4	56.7
Material per unit cost (£)	87	19.36	19.36
Sale price (£)	240	240	240

With the estimated costing in table 8, the number of units that needs to be sold to make the transition from the prototype, to the two different batch sizes, viable, can be calculated by using simultaneous equations. The coefficient of x is the total cost per unit and the y intercept (+c) is the fixed costs if you were to buy the machinery required to manufacture the parts (injection mould, welding equipment, etc). Equation 18 is for the prototype,

equation 19 is for the 5,000 batch and equation 20 is for the 30,000 batch.

$$y = 414x \quad (17)$$

$$y = -107.24x + 10,000 \quad (18)$$

$$y = -163.94 + 30,000 \quad (19)$$

**Transition from prototype to 5000 units:**

$$414x = -107.24x + 10000 \quad (20)$$

$x = 19$	(21)
----------	------

It would take 19 units sold to make a profit when transitioning to batch manufacturing 5000 units.

**Transition from 5000 units to 30,000 units:**

$$-107.24x + 10,000 = -163x + 30,000 \quad (22)$$

$x = 358$	(23)
-----------	------

It would take 358 units sold to make a profit when transition to batch manufacturing of 30,000 units. Better cost estimates need to be completed to rectify the accuracy of these calculations.

## 5.2 Manufacturing process:

### 5.2.1 Injection moulding:

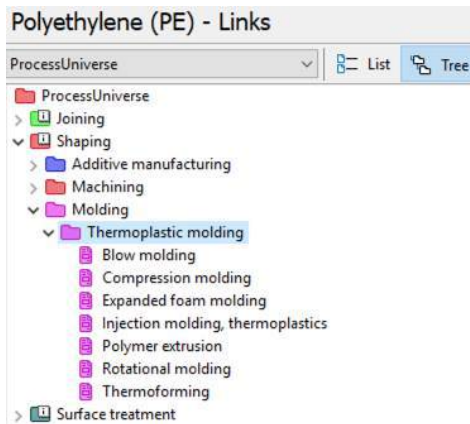


Figure 17 Manufacturing processes for PE (Granta,2021).

Out of these processes, injection moulding would be the most ideal for the components in my design. The tooling and equipment cost is very high but minimal labour is needed. It can produce parts with the mass range of 0.001-25kg and it produces parts with minimal surface roughness (Kryachek, 2004). It can also produce complex shapes which is required for the screw parts.

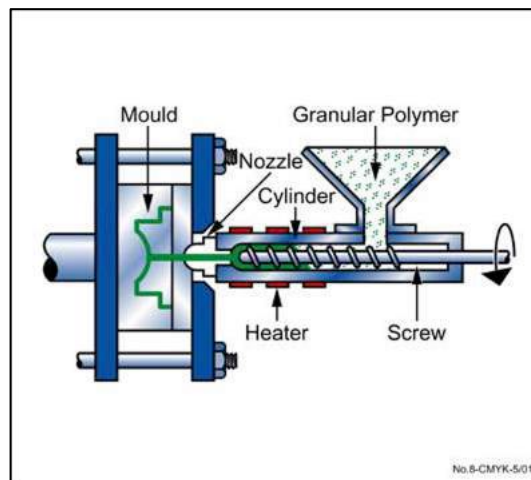
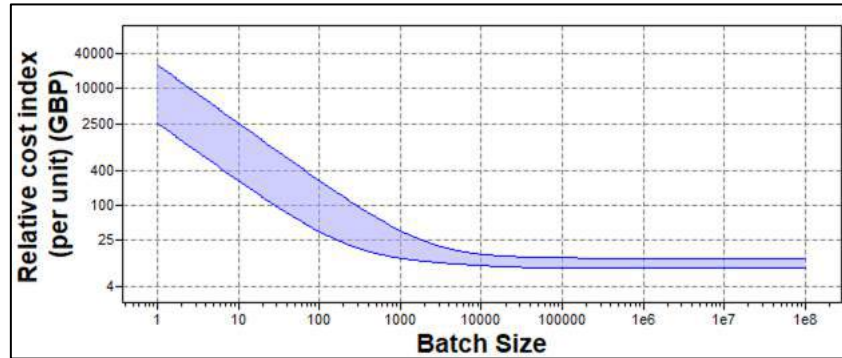


Figure 18 Injection mould.

The aim would be to produce over 10,000 of these novel water purification devices due to the population of Luanda. Graph 5 demonstrates that with large batch sizes, for a 1kg component made out of PE with a £6 material cost, the price to produce the part becomes very cheap after 10,000 units.



Graph 5 Cost VS batch size (1kg component-PE)

Further work would be required to understand a better estimate of the costing unevolved with injection moulding. For example with components area, length, thickness, a better estimate can be calculated.

## 6 Future work

One of the biggest factors for improving this water purification is reducing the design for manufacture (DFMA). Reducing the number of parts as well as the complexity of parts would greatly reduce the time and cost of manufacturing.

Further testing must be completed on the specific hollow fibre filter as to whether it is capable in sufficiently removing a faecal matter to the standards outlined by the WHO household water treatment guidelines.

Finite element analysis and CFD should also be conducted to improve the engineering design of the water purification system. Mainly improving the mechanical properties of the system. Further material should be conducted to further reduce the overall mass of the device.

### 8.3 Appendix C – Python calculations

```

1
2
3 import math
4
5
6 *****
7 Pump cylinder size calculation
8 *****
9
10 V_drum = 50 # l
11 N_pump=100 # number of pumps to empty the drum
12 k_pump_rate = 20 # Avg number of pumps per min
13 l_hose = .55 #m
14 h_cyl = .07 #m
15 D_hose = 0.005 #m
16 pump_efficiency = .90
17 design_safety_factor = 1.2
18
19 V_cyl = V_drum/N_pump
20 print('Cylinder volume: {:.3f}(l)'.format(V_cyl))
21
22 # Assuming at a rate of 20 cylinder compressions a minute, that gives an estimated volume flow rate of
23 Q_dot = (V_cyl*k_pump_rate)/60 #l/sec
24 print('Average volumetric flow rate: {:.3f}(l/min)'.format(Q_dot*60))
25 print('\t\t\t : {:.3f}(l/sec)'.format(Q_dot))
26 print('\t\t\t : {:.3E}(m^3/sec)'.format(Q_dot*1E-3))
27 Q_dot = Q_dot * 1E-3
28
29 V_cyl = V_cyl*1E-3 # conv l to m-3
30 R_cyl = math.sqrt(V_cyl/(math.pi*h_cyl))
31 print('pump cylinder radius: {:.3f}(m)'.format(R_cyl))
32
33 *****
34 Required pump pressure
35 *****
36
37 rho = 997 # kg/m^3
38 g = 9.81 #
39 lambda_p = 0.2 #0.0015 # pipe roughness for PVC
40
41
42 #m_dot = rho Q_dot = rho A V... so
43
44 m_dot = Q_dot*rho
45 print('Avg mass flow rate: {:.3f}(kg/sec)'.format(m_dot))
46
47 flow_V = m_dot/(rho * D_hose)
48 print('Avg flow velocity: {:.3f}(m/sec)'.format(flow_V))
49
50 # Pressure loss per m of pipe
51 P_loss = lambda_p *(l_hose/D_hose) * (rho/2) * flow_V**2
52
53 delta_P = rho*g*l_hose + l_hose*P_loss
54
55 print('Pressure of pump : {:.3f}(Pa)'.format(delta_P))

```

Figure 20 Pump cylinder size calculation and pump pressure.

```

57 Pump power
58 """
59
60 Pow_pump = ( Q_dot*delta_P) / pump_efficiency
61 print('Pump Avg power requirement: {:.3f}(Pa)'.format(delta_P))
62
63 """
64 Force of one pump compression
65 """
66
67 F_pump = delta_P * (math.pi * R_cyl**2) # delta_P * A_cyl
68 print('Pump force requirement: {:.3f}(N)'.format(F_pump))
69
70
71 #Because this is the required force to draw the liquid into the cylinder chamber we want this
72 # force to be acting in the opposite direction, so we load a spring instead,
73 # and use that spring to exert the force on the fluid.
74
75
76 """
77 Spring constant
78 """
79
80 k = F_pump/h_cyl
81 k_safe = (F_pump*design_safety_factor)/h_cyl
82 print('\n\nSpring constant: {:.3f}(N/m)'.format(k))
83
84 print('With a safety factor: {:2f} \n \tthis applied to account for losses and friction! \n\t spring const : {:.3f}(N/m)'
85       .format(design_safety_factor,k_safe))
86

```

Figure 21 Pump power requirement and spring constant calculations.

# WE ARE UNIVERSITY OF LIVERPOOL MOTORSPORT



210 23 22 20

Day Hrs Min Sec

[Home](#)

[News](#)

[Cars](#)

[Team](#)

[Sponsors](#)

[Competition](#)

[Contact us](#)



Built upon the foundations of IC power, we are transitioning to electric in the design and manufacture of a single-seat race car to compete at the global formula student competition.

## Silverstone, England



210

Day

23

Hrs

22

Min

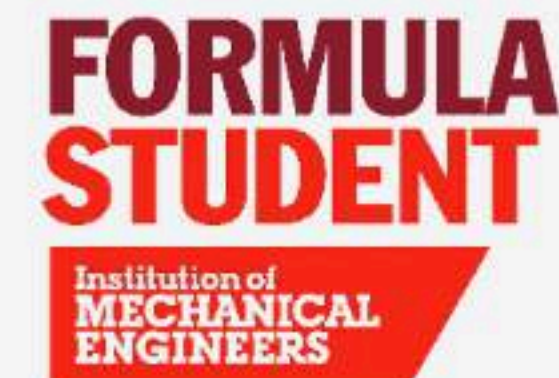
20

Sec



# Sponsors

Our success as a team is owed to our sponsors! If you would like to become a sponsor, please get in touch.





Particle Physics:  
Advanced Materials Lab



### Tweets from @ULMRacing

Follow on Twitter



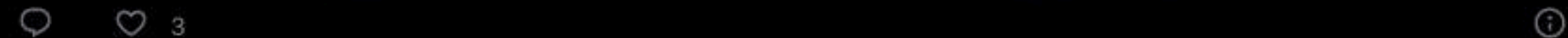
ULM Racing @ULMRacing · Nov 24

ULM015 From the Test day a few weeks ago.



Formula Student is an international competition in which top engineering students design, build and race a single seat racing car. For more information about the competition, please visit our competition page.

The team comprises a mixture of 3rd and 4th year students, allowing the years of previous experience to be passed on to



allowing the years of previous experience to be passed on to future team members. In addition to competing in Formula Student UK at the Silverstone race circuit, the team regularly attend European events including the Austrian, German and Hungarian Formula Student competitions.

## Liverpool University Motorsport



Website designed by Christopher Cooper

# OUR TIMELINE

ULM016

ULM015

ULM014

ULM013

ULM012

ULM011

ULM010

ULM009

ULM008

ULM007

ULM006

ULM005

12th of september 2021

A warm welcome back



As the team begins a fresh academic year under some strange circumstances, what better way to start than to introduce you to our Team Leader, Henry Woodward. In addition to running the whole operation and providing us all with a burning desire to succeed, Henry is now working on elements of the drivetrain.





ULM014

ULM009

ULM013

ULM012

ULM011

ULM010

ULM009

ULM008

ULM007

ULM006

ULM005

ULM004

ULM003

ULM002

ULM001

12th of september 2021

A warm welcome back



As the team begins a fresh academic year under some strange circumstances, what better way to start than to introduce you to our Team Leader, Henry Woodward. In addition to running the whole operation and providing us all with a burning desire to succeed, Henry is now working on elements of the drivetrain. Lorem ipsum dolor sit amet consectetur adipisicing elit. Iste adipisci at totam voluptas? Labore, recusandae aliquam nam enim libero ipsa architecto quis sed reprehenderit sit, quasi est ducimus optio molestiae!



As the team begins a fresh academic year under some strange circumstances, what better way to start than to introduce you to our Team Leader, Henry Woodward. In addition to running the whole operation and providing us all with a burning desire to succeed, Henry is now working on elements of the drivetrain.





Silverstone, England

210 23 30 59  
Day Hrs Min Sec

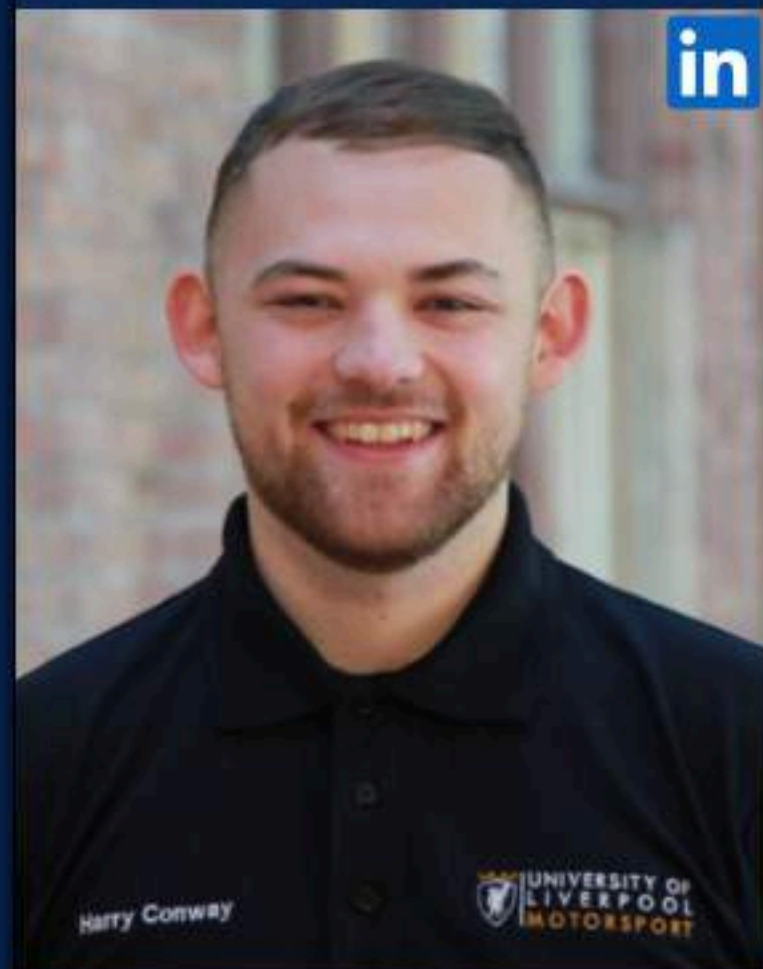
- Home
- News
- Cars
- Team
- Sponsors
- Competition
- Contact us

# WELCOME TO THE TEAM



## Team members

Harry Conway



**Team Leader**

EV systems

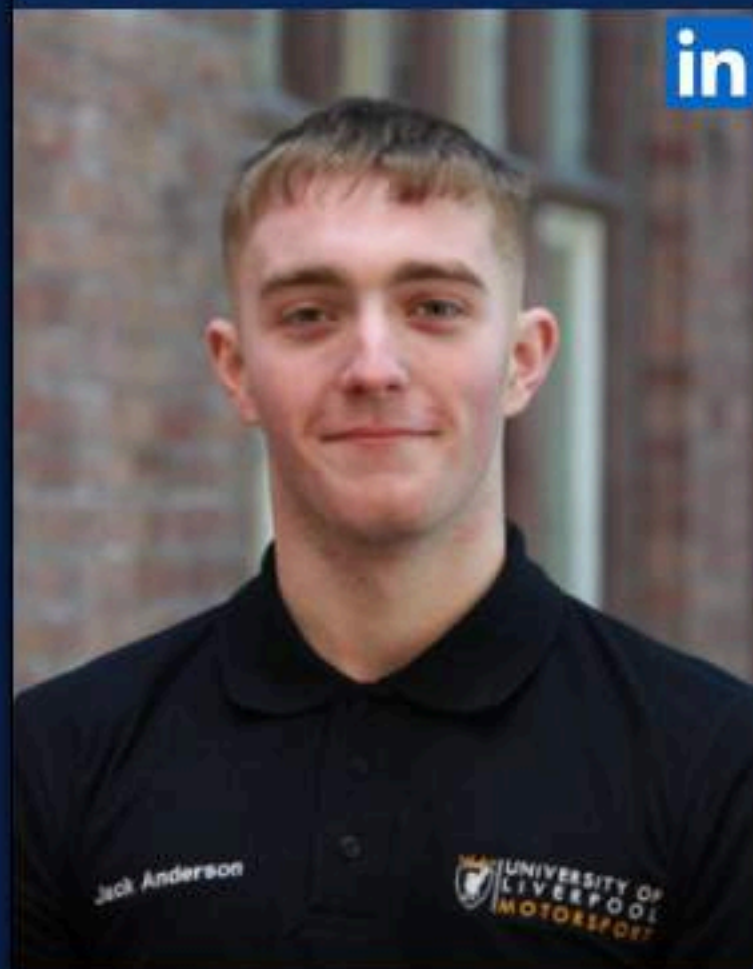
Joshua Lacey



**Deputy Team Leader**

Chassis

Jack Anderson



**Y3 Manager**

EV systems

Zac Adams



**Marketing Manager**

EV systems

Alasdair Blain



**Social Manager**

EV systems

Ewan Darlington



**Driving Manager**

Powertrain

Jorge Garcia Llopis



Matt Hutton



Georgios Lamprou



Anna Martindell



Krishan Mistry



Jithin Roy











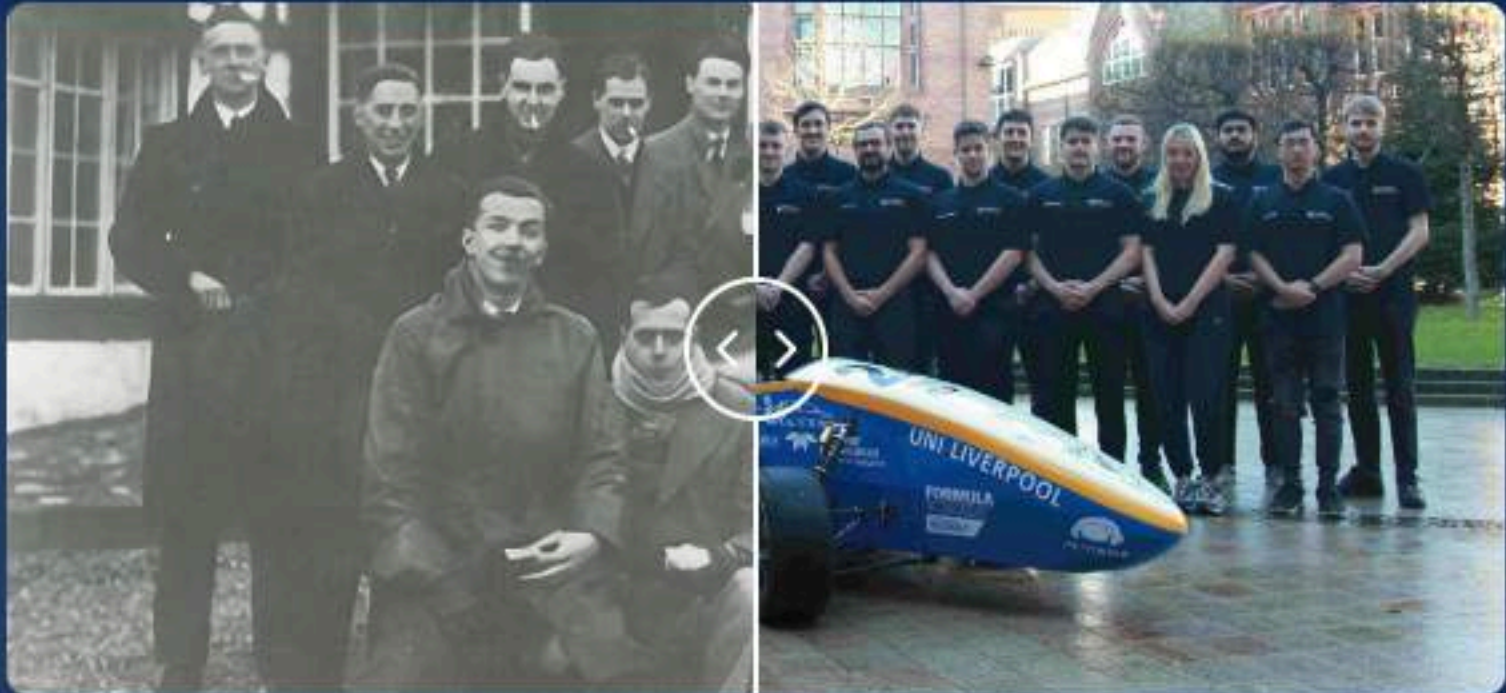
## Liverpool University Motorsport



Website designed by Christopher Cooper



## WE ARE UNIVERSITY OF LIVERPOOL MOTORSPORT



Built upon the foundations of IC power, we are transitioning to electric in the design and manufacture of a single-seat race car to compete at the global formula student competition.

### Silverstone, England



**210**

**Day**

**23**

**Hrs**

**14**

**Min**

**17**

**Sec**

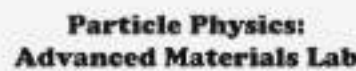


## Sponsors

Our success as a team is owed to our sponsors! If you would like to become a sponsor, please get in touch.



SPONSORS, PLEASE GET IN TOUCH!





## Tweets from @ULMRacing

Follow on Twitter



ULM Racing @ULMRacing · Nov 24



ULM015 From the Test day a few weeks ago.





3



**ULM Racing** @ULMRacing · Sep 12



University of Liverpool Motorsport is looking for potential sponsors for the 2023 Formula Student UK event. To find out more about us please follow the link to our website: [ulm.FormulaStudent.org.uk/home.html](http://ulm.FormulaStudent.org.uk/home.html)



Formula Student is an international competition in which top engineering students design, build and race a single seat racing car. For more information about the competition, please visit our competition page.

The team comprises a mixture of 3rd and 4th year students, allowing the years of previous experience to be passed on to future team members. In addition to competing in Formula Student UK at the Silverstone race circuit, the team regularly attend European events including the Austrian, German and Hungarian Formula Student competitions.

## Liverpool University Motorsport



Website designed by Christopher Cooper



# OUR TIMELINE

**12th of september 2021**

**A warm welcome back**

ULM016

ULM015

ULM014

ULM013

ULM012

ULM011

ULM010

ULM009

ULM008

ULM007

ULM006

ULM005

ULM004



As the team begins a fresh academic year under some strange circumstances, what better way to start than to introduce you to our Team Leader, Henry Woodward. In addition to running the whole operation and providing us all



# ULM012

12th of september 2021

A warm welcome back



As the team begins a fresh academic year under some strange circumstances, what better way to start than to introduce you to our Team Leader, Henry Woodward. In addition to running the whole operation and providing us all with a burning desire to succeed, Henry is now working on elements of the drivetrain. Lorem ipsum dolor sit amet consectetur adipiscing elit. Iste adipisci at totam voluptas? Labore, recusandae aliquam nam enim libero ipsa architecto quis sed reprehenderit sit, quasi est ducimus optio molestiae!





WELCOME TO THE TEAM



## Team members

**Harry Conway**



**Team Leader**

**Joshua Lacey**



**Deputy Team Leader**

**Jack Anderson**



**Y3 Manager**



**EV systems**

**Chassis**

**EV systems**

**Zac Adams**



**Marketing Manager**

**EV systems**

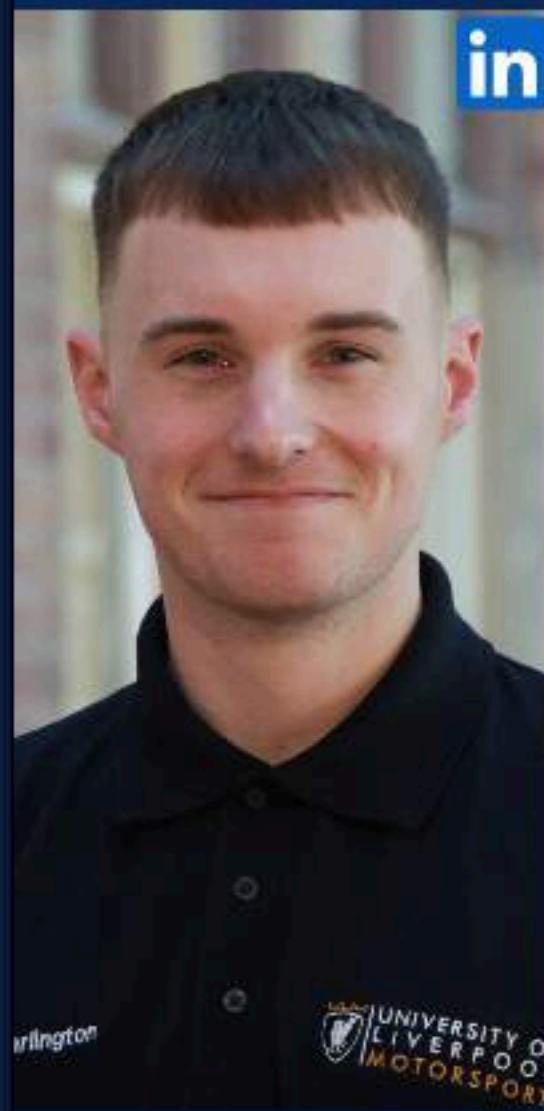
**Alasdair Blain**



**Social Manager**

**EV systems**

**Ewan Darlington**



**Driving Manager**

**Powertrain**

**Jorge Garcia Llopis**



**Matt Hutton**



**Georgios Lamprou**





**Driver Manager**  
**Special Projects**



**Sponsorship Manager**  
**Chassis**



**Design Manager**  
**Suspension & Steering**

**Anna Martindell**



**EV Operations Manager**  
**EV Systems**

**Krishan Mistry**



**Compliance Manager**  
**Special Projects**

**Jithin Roy**



**EV Compliance Manager**  
**Brake System**







## Liverpool University Motorsport



Website designed by Christopher Cooper